EXPERIMENTAL INVESTIGATION OF THE PERFORMANCE OF A BUILDING INTEGRATED THERMAL SOLAR COLLECTOR FOR DOMESTIC WATER HEATING

A thesis

submitted in fulfilment

of the requirements for the degree

of

Master of Engineering

at

The University of Waikato

by

WILLIAM TOU'ANGA ROHORUA

THE UNIVERSITY OF
WAIKATO
Te Whare Wānanga o Waikato

2013

“*Have the courage to follow your heart and intuition. They somehow already know what you truly want to become. Everything else is secondary.”*

Steve Jobs

ABSTRACT

The recent increased interest in renewable energy has created a need for research in the area of solar technology, particularly solar water heating collectors and systems. In this study a new design of a building integrated thermal (BIT) collector was developed and experimentally tested. The subsequent result of this was the viability of its use in a water heating system for domestic application in a country like New Zealand, can be investigated.

Experimental results showed that the unglazed and glazed collector can achieve thermal efficiencies of 39% and 75%, respectively. A comparison of the glazed BIT with an integrated collector of a similar design showed that the maximum thermal efficiency of 75% was relatively high; however, the downside to this is that high losses also occurred.

A theoretical viewpoint of the collector showed that the improvement in efficiency was attributed to the high fin efficiency which resulted from using a high thermal conductivity material relative to the integrated collector previously studied. Moreover, the high heat loss from the collector was shown to be a result of the lack of side insulation and the presence of air gaps between the collector and the rear insulation, contributing to the overall heat loss from the collector and system.

A control strategy was also developed for the control of the system and simulated tests showed that the controller was indeed effective in controlling the system. However, it was highlighted that an improvement is needed for the method of simulating the load required by the household. Additionally, transient simulation of the developed system showed that accurate predictions of the systems performance can be made. Moreover, using a hypothetical scenario where the heat loss from the BIT collector-system is reduced, it was shown that a significant improvement in its performance for water heating can be made.

This work has shown that the use of integrated collectors for domestic household heating in New Zealand is indeed viable. The potential for the control of these systems to achieve high efficiencies is also recommended, by using advance control strategies.

ACKNOWLEDGEMENTS

First and foremost I would like to express my gratitude to Prof. John Gibson and his colleagues from the Waikato Management School for providing me with the scholarship for this study. Thank you also, to Dr. Mike Duke for allowing me to undertake this work.

Sincere thanks to the technicians and plumber who have contributed to the development of the experimental systems. In a heavily experimental work such as this, there are too many to name, but do know that your help has been greatly appreciated. To my fellow postgraduate colleagues and administrative staff at the Faculty of Science and Engineering, my sincere thanks.

I owe the most, however, to my parents, Dr. Halahingano and Dr. Frederick Rohorua, the man I am today is a direct reflection of the sacrifices you have both made. Know that your love and support will forever be appreciated as I begin a new chapter of my life. This also extends to my siblings, my brothers, Mac, Joe and Tevita and sister in law, Lea. Toooo much!

Finally to my wife, Jaleese, who has been my foundation during my time at the university and to our two beautiful children, Jaylam and Torez, this thesis I dedicate to you. To each and everyone my sincere thanks. Errors and weakness however, remain my own responsibility.

TABLE OF CONTENTS

LIST OF FIGURES

LIST OF TABLES

NORMENCLATURE

A	Collector area (m^2)
A_G	BIT gross collector area (m^2)
C_b	Bond conductance
C_p	Specific heat (J/kgK)
D	Tube diameter (m)
D_i	Tube inner diameter (m)
d_h	Hose diameter (m)
F	Fin efficiency
F'	Collector efficiency factor
F_R	Collector heat removal factor
f	Solar fraction
G	Incident radiation (W/m^2)
G_T	Global irradiance (W/m^2)
h_{fi}	Collector fluid internal heat transfer coefficient (W/m^2K)
h_w	Wind induced heat transfer coefficient (W/m^2K)
k_A	Absorber conductivity (W/mK)

k_{in}	Insulation conductivity (W/mK)
L	required load (MJ/hr)
L_c	Collector length (m)
L_{in}	Backing insulation thickness (m)
L_s	Supplied load (MJ/hr)
M	Fin efficiency absorber thermal conductivity parameter
m	Mass flow rate (kg/s)
N	Number of glazing layers or covers
n	Number of tubes
P_{max}	Pump maximum power (W)
p_{max}	Drain-back maximum working pressure (kPa)
$Q_{collector}$	BIT collector heat input (W)
Q_i	Collector heat input (W)
Q_o	Rate of heat loss (W)
Q_{tank}	Tank heat output (W)
Q_u	Useful or actual heat input (W)
R	Thermal resistance (R-value) (Km^2/W)

T	Temperature (K)
T_a	Ambient temperature (K)
T_c	Collector average temperature (K)
T_{ci}	BIT collector inlet temperature (K)
T_{co}	BIT collector outlet temperature (K)
$T_{element}$	Tank element temperature (K)
T_{exit}	Tank outlet temperature (K)
T_i	Collector inlet temperature (K)
T_{main}	Tank inlet temperature (K)
T_o	Collector outlet temperature (K)
T_{tank}	Tank cold region temperature (K)
T_{t1}	Tank hot region temperature (K)
T_{t2}	Tank level two temperature (K)
T_{t3}	Tank level three temperature (K)
t	Absorber thickness (m)
t_{loss}	Tank standing heat loss (kWh/d)
$(UA)_{edge}$	Edge loss coefficient-area product

U_e	Edge loss coefficient (W/m^2K)
U_L	Collector total heat loss coefficient (W/m^2K)
V_{db}	Drain-back tank volume (L)
V_{st}	Storage tank volume (L)
W	Tube spacing (m)
w_c	BIT collector width (m)

Greek

α	Absorptance
β	Collector mounting angle (degrees)
Δ	Temperature difference
η	Collector efficiency
η_G	Instantaneous collector efficiency
η_0	Collector optical efficiency
τ	Transmittance
$\tau\alpha$	Transmittance-absorptance product

Chapter 1: Introduction

1.1 Overview

The world has seen many significant developments that have had an impact, both directly and indirectly on renewable energy. Renewable energy comes from natural resources such as sunlight, wind, rain, tides, and geothermal heat, which are naturally replenished. In recent years concern has grown over the use of non-renewable energy such as coal, oil and natural gas and particularly the environmental effects and unsustainable nature of these energy sources (Tian and Zhao, 2013).

Improvements in quality of life and rapid industrialisation in many countries are increasing energy demand significantly and the potential future gap between energy supply and demand is predicted to be large (Tian and Zhao, 2013). As a result, interest in sustainable development has continued to grow, motivating the development of environmentally friendly energy technologies. More specifically, research into the applications of solar energy technologies has as a consequence expanded rapidly, exploiting the abundant, free and environmentally benign characteristics of solar energy (Kumar and Rosen, 2011).

Despite this, widespread acceptance of solar energy technology still depends on its competitiveness with traditional non-renewable energy, considering factors such as reliability and cost-effectiveness (Kumar and Rosen, 2011).

1.2 Solar Energy

Solar energy is the most abundant of all energy resources. Indeed, the rate at which solar energy is intercepted by the Earth is about 10,000 times greater than the rate at which humankind consumes energy (Arvizu et al., 2011).

The Earth receives around 174 x 10^{14} kW of incoming solar radiation at the upper atmosphere. It is well known however, that approximately 30% is reflected back to space while the rest is absorbed by clouds, oceans and land masses (Kreith and Goswami, 2007). The total solar energy absorbed by Earth's atmosphere, oceans and land masses is approximately 3.9 million EJ per year. The amount of solar energy reaching the surface of the planet is so vast that in one year it is about twice as much as will ever be obtained from all of the Earth's non-renewable energy resources combined (Weston A, 2006). This highlights why solar energy has received more interest than other forms of renewable energy, principally because it has the potential to generate all of the world’s energy requirements many times over (Kreith and Goswami, 2007).

Solar energy conversion consists of a large family of different technologies capable of meeting a variety of energy service needs. Solar technologies can deliver heat, cooling, natural lighting and electricity for a host of applications.

Conversion of solar energy to heat is comparatively straightforward, because any material object placed in the sun will absorb thermal energy. However, maximising that absorbed energy and inhibiting losses to the surroundings can take specialised techniques and devices. The technique employed is largely dependent on the application and temperature required. This can range from 25°C

(e.g., for swimming pool heating) to 1,000°C (e.g., for dish/Stirling concentrating solar power) and even up to 3,000°C in solar furnaces (Edenhofer et al., 2011).

Passive solar heating is a technique for maintaining comfortable conditions in buildings by exploiting the solar irradiance incident on the buildings through the use of glazing (windows, sun spaces, conservatories) and other transparent materials and managing heat gain and loss in the structure without the dominant use of pumps or fans.

Solar cooling for buildings can also be achieved, for example, by using solar-derived heat to drive thermodynamic refrigeration absorption or adsorption cycles. Solar energy for lighting on the other hand, actually requires no conversion since solar lighting occurs naturally in buildings through windows. However, maximising the effect requires specialised engineering and architectural design (Edenhofer, et al., 2011).

Generation of electricity can be achieved in two ways. The first, more traditional method converts solar energy directly into electricity using a device called a photovoltaic (PV) cell. In the second, solar thermal energy is used in a concentrating solar power (CSP) plant to produce high-temperature heat, which is then converted to electricity via a heat engine and generator (Lovegrove and Stein, 2012).

1.3 Solar Energy in New Zealand

Generally, it is well known that sunlight can reach the Earth's surface with a maximum intensity of more than 1,000 watts per square metre. Although not all countries are equally endowed with solar energy, a significant contribution to the energy mix from 'direct' solar energy is possible for almost every country (Arvizu, et al., 2011).

In New Zealand for example, the annual sunshine hours ranges from about 1,600 in Invercargill to over 2,400 in Blenheim, and the main centres receive about 2,000 hours. While the total household rooftop area in New Zealand is exposed to solar energy that equates to about twice the total national energy use, the resource is relatively low in intensity for much of the day and available only intermittently (Meduna, 2013).

A report by the Energy Efficiency and Conservation Authority (EECA, 2009), henceforth referred to as EECA, has shown that conventional electric water heating systems are the biggest energy consumers in most New Zealand households, making up around 40% of the power bill. While solar water heating (SWH) systems do not produce any electricity directly, they replace the use of considerable amounts of natural gas or electricity that are produced at least partly from non-renewable fossil fuels. EECA go on to say that the average rooftop of a New Zealand house collects about 50 times as much energy from solar as is required for water heating. This translates to a SWH system supplying around 50 to 75% of the annual water heating energy requirement when installed correctly.

In most New Zealand locations, a SWH system can produce up to 15 kWh per day in summer, more than enough for an average four-person household. But in winter it only provides around 9 kWh, less than half the daily requirement (EECA, 2009). Therefore such systems generally have to be backed up by electricity, gas or wood burner water-heaters. This is largely due to the fact that there is an increase in hot water consumption during winter periods compared to summer. Additionally, compared to summer, there are lower levels of solar radiation during winter; this along with relatively low ambient conditions reduces the amount of energy that can be gained by solar energy technologies (Anderson, 2009).

The Solar Association of New Zealand (SANZ, 2011) stated that New Zealand provides more than 40 GWh of equivalent electricity consumption per year through the use of SWH. They go on to say that by 2010, it is widely thought this figure could be upwards of 600 GWh per year. They conclude by saying that the potential for solar energy use in New Zealand is promising, indicating that the total amount of solar energy that the New Zealand land mass collects is approximately 400 million GWh per year. Each year around 1,800 solar water units are installed, mostly in single family homes, this clearly highlights the growth in demand as the benefits are recognised (Meduna, 2013).

1.4 Solar Water Heating Systems Overview

Hot water heating for domestic and commercial buildings is now a mature technology growing at a rate of about 16% per annum and employed in most countries of the world (Edenhofer, et al., 2011). The world installed capacity of SWH systems at the end of 2010 has been estimated to be 185 GWth (giga watts-thermal) (Raisul Islam et al., 2013). Of particular interest is the application of SWH systems in the domestic sector. A report by the International Energy Agency Solar Heating and Cooling programme (Weiss and Mauthner, 2012) showed that SWH systems contributed 85% of the total installations at the end of 2010, as shown in Figure 1. In New Zealand, SWH systems for single family homes contributed 95% of the total for solar thermal systems, as shown in Figure 2.

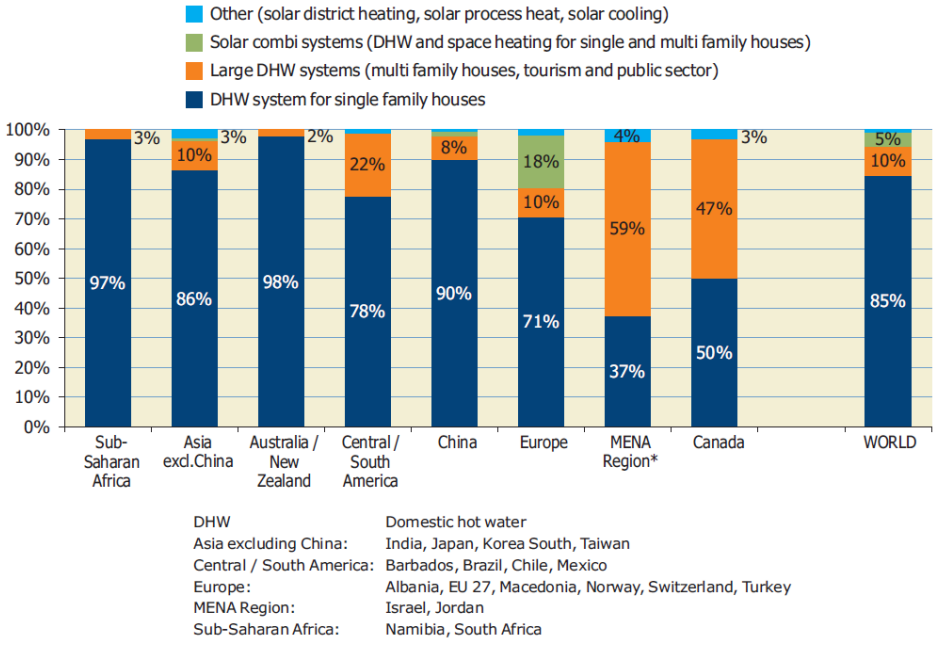

Figure 1: Distribution of solar thermal systems by application for the total installed glazed water collector capacity in operation by the end of 2010 (adapted from, Weiss and Mauthner, 2012).

Country	Reference climate	Collector area (gross area) for single sys. [m²]	Total collector area-SFH 2010 [m²]	Share of DHW-SFH [%]	Total number of systems SFH 2010 [-]	Type of system [-]
Albania	Tirana	2,5	22.543	29%	9.017	TS
Australia	Sydney	6,0	2.857.251	98%	476.209	PS
Austria	Graz	6,0	1.858.739	47%	309.790	PS
Barbados	Grantley Adams	4,0	131.690	100%	32.923	TS
Belgium	Brussels	4,0	316.634	100%	79.159	PDS
Brazil	Brasília	4,0	4.157.540	86%	1.039.385	TS
Bulgaria	Sofia	4,0	33.306	71%	8.327	PS
Canada	Montreal	6,0	33.107	50%	5.518	PS
Chile	Santiago de Chile	4,0	12.953	46%	3.238	PS
China	Shanghai	4,0	151.200.000	90%	37.800.000	TS
Cyprus	Nicosia	4,0	786.811	87%	196.703	TS
Czech Republic	Prague	6,0	178.605	58%	29.767	PS
Denmark	Copenhagen	4,0	455.708	86%	113.927	PS
Estonia	Tallinn	4,0	2.841	100%	710	PS
Finland	Helsinki	4,0	32.738	95%	8.184	PS
France incl. DOM	Paris	4,0	1.645.272	75%	411.318	PS
Germany	Wurzburg	6,0	5.887.419	45%	981.237	PS
Greece	Athens	2,5	4.005.260	98%	1.602.104	TS
Hungary	Budapest	6,0	74.907	50%	12.485	PS
India	Delhi	4,0	3.176.000	80%	794.000	TS
Ireland	Dublin	4,0	136.059	90%	34.015	PS
Israel	Jerusalem	4,0	827.579	20%	206.895	TS
Italy	Bologna	4,0	2.547.578	100%	636.895	PS
Japan	Tokyo	4,0	5.175.606	98%	1.293.901	TS
Jordan	Amman	4,0	790.050	80%	197.512	TS
Korea, South	Seoul	4,0	845.812	54%	211.453	PS
Latvia	Riga	4,0	7.244	100%	1.811	PS
Lebanon	Beirut	4,0	348.312	100%	87.078	TS
Lithuania	Vilnius	4,0	4.518	100%	1.130	PS
Luxembourg	Luxembourg	4,0	30.800	100%	7.700	PS
Macedonia	Skopje	4,0	12.100	47%	3.025	PS
Malta	Luqa	4,0	43.469	100%	10.867	PS
Mexico	Mexico City	4,0	243.561	28%	60.890	PS
Morocco	Rabat	4,0	341.260	100%	85.315	TS
Namibia	Windhoek	4,0	9.903	45%	2.476	TS
Netherlands	Amsterdam	3,0	331.857	80%	110.619	PDS
New Zealand	Wellington	4,0	144.989	95%	36.247	PS
Norway	Oslo	6,0	15.151	98%	2.525	PS
Poland	Warsaw	6,0	459.060	70%	76.510	PS

DHW-SFH: domestic hot water systems
TS: thermosiphon system
Auxiliary heating device: oil boiler

PS: pumped system for single-family houses
PDS: pumped drain back system

Figure 2: Domestic hot water reference systems for single family houses and the total collector area in operation by the end of 2010 (adapted from, Weiss and Mauthner, 2012).

A SWH system consists essentially of a collector for receiving solar radiation which is used to heat the fluid connected to a storage tank by pipes. Traditionally there are two types of collectors available which are flat plate and evacuated tube collectors. Flat plate collectors are the most extensively used of the two, due to its relatively low cost, simple design and high efficiencies (Duffie and Beckman, 2006; H.P. Garg, 1987; Kreith and Kreider, 1978).

A typical diagram of a passive (left) and active (right) SWH system is shown in Figure 3. For the passive system the water in the riser tubes gets heated by 'insolation' (the absorption of solar radiation), it flows upwards into the upper header tube and from there into the top of the insulated storage tank, pushing down the colder water to the bottom of the tank through the connecting pipe into the lower header tube. This natural flow of water by a form of convection or thermosyphon process ensures that heat keeps flowing from the fins of the absorber (which has a black coating for better absorption of radiation) into the water contained in the risers.

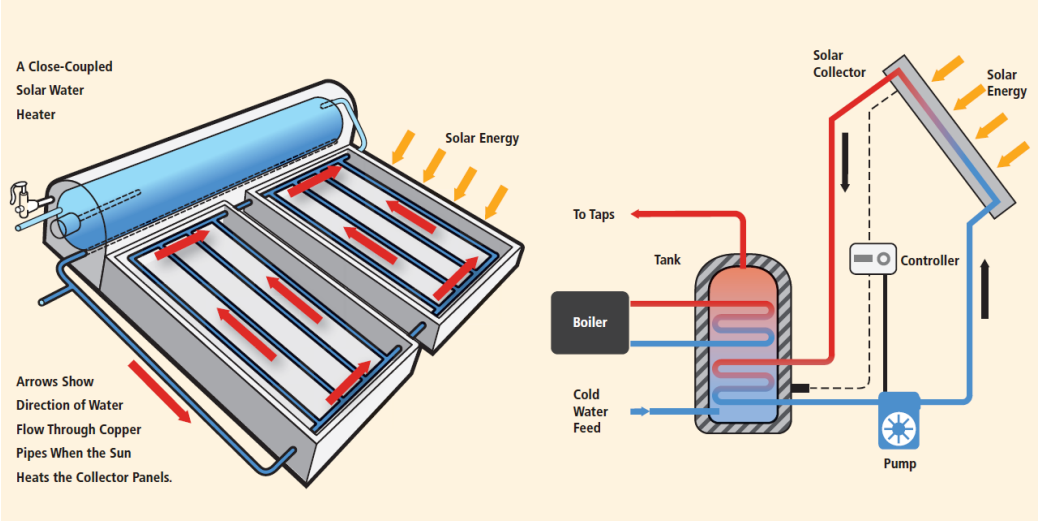

Figure 3: Generic schematics of solar thermal system, left: Passive (thermosyphon), right: Active (adapted from, Arvizu, et al., 2011).

For large systems the length of the pipes connecting the collectors to the tank or tanks becomes so great that the pressure drop across the system makes it impossible to use the thermosyphon process (Kalogirou, 2009). To circumvent this, a small electrical pump has to be provided to maintain a forced circulation. For a fixed collector, the collector is mounted on a horizontal surface, usually a roof, at a slope of 10° greater than the local latitude so that it receives optimum

incident solar radiation during the winter months when the hours of sunlight are least. This isn't needed if the collector is fitted with a tracker which adjusts its inclination according to the suns movement relative to the collector location. These complicated devices are generally restricted to large solar thermal power plants (Lovegrove and Stein, 2012).

Both the absorber and the storage tank must be well insulated, the former so that the solar radiation received goes entirely into heating the water and the latter so that heat loss from the hot water during both day and night is minimised. The glass cover of the collector ensures that radiation is received by the absorber but very little is lost (since glass is opaque to the far infrared radiation emitted by a warm body, the greenhouse principle).

The performance of the whole system depends on the choice of materials, important factors being the thermal conductance of the absorber tubes and fins, the efficacy of the bonding between tubes and fins, the quality of the insulation, and the corrosion resistance of the entire system, bearing in mind that some parts are exposed to water (of variable purity) at moderately high temperatures and most of the remaining components have to withstand sun and humid air (Raisul Islam, et al., 2013).

1.4.1 SWH Technology and Evaluations

Even though the use of solar energy for water heating and other low end applications is centuries old, the SWH system in the present form was designed, developed and investigated initially by Close, 1962, Bhardwaj et al., 1967 and Gupta and Garg, 1968. In New Zealand, following on from the oil shocks of the 1970s, interest in SWH systems was high. In the 1978 Budget, the Maldoon Government introduced an interest-free load scheme for SWH's which required rules around how systems would be approved to qualify for the scheme (Synergy Applied Research, 1985). A component of this was detailed product testing by the then, Department of Scientific and Industrial Research (DSIR) following specific testing procedures. (A range of results are provided in Synergy Applied Research, 1985).

It began to emerge that the performance of SWH's in actual operation (i.e. in-situ) was less than that determined by following the specific testing procedures. However, by the time Synergy Applied Research proposed an in-situ measurement programme in 1986 (Synergy Applied Research, 1986), interest in SWH's had declined, oil prices had dropped and government programmes were out of favour.

During this period, progress continued on testing standards. An important component of this was the development and validation of computer simulation programmes such as TRNSYS (Solar Energy Laboratory (SEL), 2008). These programmes could reliably predict the performance of SWH systems from component measurements, reducing the cost of testing and providing tools to improve system design. Extensive work has been undertaken at the University of

New South Wales (UNSW) on adapting these programmes for Australian conditions (Morrison, 2012). The joint Australian and New Zealand Standard AS/NZS: 4234 is a good example of a standard which "provides the means of evaluating the annual task performance of heated water systems" for both Australian and New Zealand climate zones. The performance evaluations outlined in the standard are based on modelling annual performance using the TRNSYS software for a range of climatic conditions in both countries.

1.4.2 Whole System Performance

An early in-situ project involved the monitoring of 12 SWH systems in a solar village development in Sydney around 1984 (Morrison et al., 1984), where it was found that energy savings of 50% or more were obtained in nine of the 12 systems. A more recent study (Lloyd, 2001), examined the performance of 33 water heating systems in remote indigenous communities around Australia and considered a range of technologies such as SWH and heat pump water heating (HPWH) systems. They found that there was a wide range in the performance of the systems which was caused by the extreme variation in water use within these communities.

These results were also found in a series of laboratory-based performance measurements on a number of SWH (and HPWH) systems in the University of Otago (Thomas and Lloyd, 2005). Large differences in the performance of the different types of systems were found. Around the same time, an analysis of some of the half dozen SWH systems that were part of the households in the Household

Energy End-use Project (HEEP) sample raised some concerns about how these systems were being managed by householders or end-users (Pollard et al., 2005).

An immediate predecessor to this project was the report by Stoecklein (2005), which looked to examine the cost-effectiveness of SWH systems, and highlighted the lack of verified field performance measures underpinning the financial analysis. Pollard and Zhao (2008) also found that the overall energy performance of 35 SWH systems installed between 2004 and 2006 in New Zealand, varied considerably and included a number of systems which they considered 'poorly-performing.'

In terms of the influence of seasonal variation on the performance of SWH (and HPWH), Lloyd and Kerr (2008) found that the heat pump system was more likely to result in a better match when considering security of supply, greenhouse gas (GHG) emissions and reduced peak transmission loading compared to the solar option. Carrington (2011) however, analysed different SWH (and HPWH) systems against referenced systems as set out in the AS/NZS4234 standard and found that the annual electricity savings "are not significantly affected by realistic changes in the daily hot water consumption pattern." Moreover, increasing annual electricity savings (kWh) for both types of systems were observed when increasing water demand. The author however, noted that "a single performance measure, such as the percentage annual savings for a particular consumer in a defined climate zone, cannot represent the relative contributions of the systems to sustainable energy, supply security and lower costs."

These studies have shown that although there are standardised test methods for evaluating the performance of SWH systems, there are large variations in system performances when considering the same systems in-situ. This is because the systems are subject to the vagaries of daily hot water consumption patterns and environmental conditions, which in most cases vary from household to household. This view is shared by Shariah and Ecevit (1995), who noted that for thermo-siphon systems "generally the performance of the thermo-siphon system is given in terms of the instantaneous efficiency on clear days. However this does not give the true long term performance of the system because of varying climatic and radiation conditions."

1.4.3 Other Aspects of SWH

Other aspects of SWH systems include the control systems for both heating and fluid flow and the performance of other components apart from the collector, such as the storage tank. In terms of the user interaction, Prud'homme and Gillet (2001) suggested that current control strategies for SWH systems "do not take into account the evolution of the operational conditions, typically the users' needs in terms of draw off and the weather conditions." Importantly, the implementation of control strategies to manage the electric boost that is typically used on many systems has not been a high priority by either system designers or manufacturers. The priority has been on maximizing energy transfer from solar radiation to the storage tank on a given day. The theory at least is that provided there is good thermal stratification in the storage tank and the boost element and thermostat are placed between half way and a third of the way from the top of the tank, then the energy from the boost element will not interfere with solar collection.

Unfortunately there is some evidence that satisfactory thermal stratification may not be always achieved in practice. Jordan and Furbo (2005) note that the stratification depends "on the flow rate, the draw off volume as well as the initial temperature in the storage tank".

Other factors include the orientation of the tank (either vertical or horizontal), the presence of an effective diffuser on the cold water inlet, the flow rates for circulating pumped systems and the geometry and configuration of the boost element. With little or no thermal stratification, a solar hot water system utilising a simple thermostat control is likely to perform badly, particularly when draw-off occurs either in the evening or early morning, as the boost will turn on and heat the water in the storage tank by the time the sun is high enough in the sky to allow solar collection. It has also been shown that stratified tanks have some tendency to destratify over time due to diffusion and wall conduction (Lavan and Thompson, 1977).

It has been stated elsewhere (Duffie and Beckman, 2006), that the degree of stratification in a 'real' tank will depend on the design of the tank; considering factors such as the size, location, design of the inlets and outlets and the flow rates of the entering and leaving streams. It has been shown however that it is possible to design tanks with low inlet and outlet velocities that result in a highly stratified tank (Gari and Loehrke, 1982 and van Koppen et al., 1979). Shariah and Löf (1997) however, looked at four different daily consumption profiles and found that when water was drawn off during the evening and morning the efficiency of the system was reduced. Furthermore, they found that randomly timed draw offs over a 24 hour period gave the best overall system performance. It should be

noted here that if solar collector panels are retrofitted to existing storage tanks it is unlikely that the positions of the control thermostat, panel return line, the boost element or the cold water intake diffuser can be modified to optimally suit solar energy collection.

1.5 Collector Overview

Literature on SWH systems has shown that there a numerous areas for which specific works can be applied. A more predominant area has been the focus on collector performance. This is the key component in the heat transfer process on the solar side of SWH systems because it deals with the direct conversion of solar energy into thermal energy required for heating. As stated above the two traditional types of collectors used in SWH systems are the evacuated tube and flat-plate collectors, the latter being the most common.

1.5.1 Flat-Plate Collectors

A typical flat-plate collector consists of an absorber, transparent cover sheets and an insulated box, as shown in Figure 4. The absorber is usually a sheet of high-thermal conductivity metal with tubes or ducts either integral or attached. Its surface is painted or coated to maximise radiant energy absorption and in some cases to minimise radiant emission. The insulated box provides structure and sealing and reduces heat loss from the back or sides of the collector (Kalogirou, 2004).

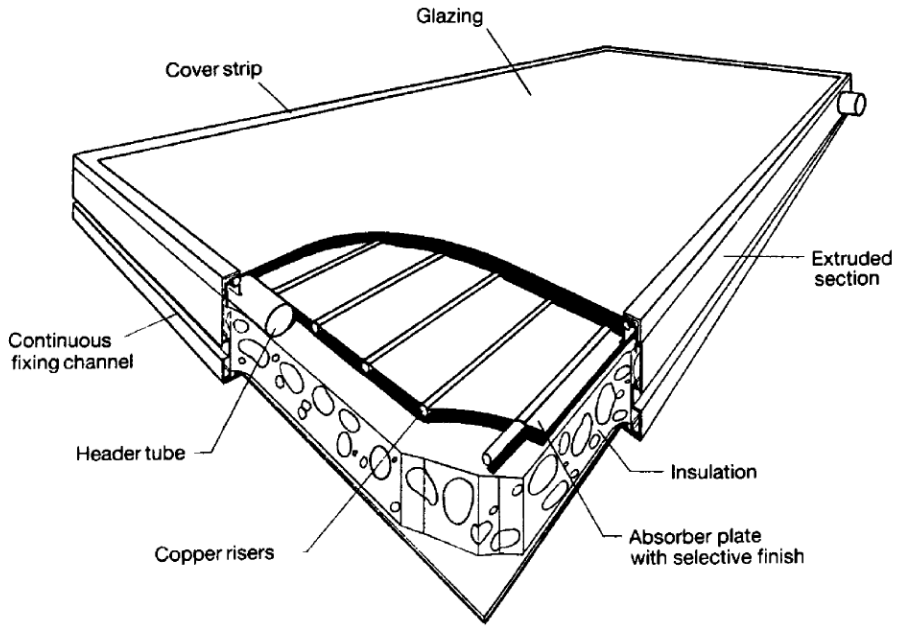

Figure 4: Configuration of a typical flat-plate collector (adapted from, Kalogirou, 2004).

The most widely used method of evaluating the performance of flat plate collectors has been the thermal energy analysis. This performance evaluation relies on the energy balance of the collector in steady state, which indicates the distribution of incident solar energy into useful energy gain, thermal losses and optical losses.

If G is the intensity of the solar radiation, in W/m^2, incident on the aperture plane of the solar collector with a collector surface area of A, in m^2, then the amount of solar radiation received by the collector can be expressed using Equation 1 (Cox and Raghuraman, 1985).

$$Q_i = GA \tag{1}$$

Where, Q_i is collector heat input in W.

However, this equation doesn't account for the losses caused by the reflection of radiation back to the atmosphere. If glazing is used, this absorbs another component and is transferred through it to the absorber plate as short wave radiation. Therefore, the percentage of the solar radiation, which penetrates the transparent cover of the collector and the percentage of radiation being absorbed, is indicated by a conversion factor. Basically, it is the product of the rate of transmission of the cover and the absorption rate of the absorber, Equation 1 is then modified to account for this and shown in Equation 2.

$$Q_i = G\,(\tau\alpha)\,A \tag{2}$$

Where, $\tau\alpha$ is the transmission and absorption coefficient of the glazing and plate

As the collector absorbs heat, its temperature becomes higher than that of the surrounding and thermal energy is transmitted to the atmosphere through convection and radiation. The rate of heat loss, Q_o is dependent on the overall heat transfer coefficient, U_L, of the collector and its temperature. The rate of heat loss, Q_o, can be expressed by Equation 3.

$$Q_o = U_L\,A\,(T_c - T_a) \tag{3}$$

Where, Q_o is heat loss, W, U_L is the collector overall heat loss coefficient in W/m^2, T_c and T_a is the collector average temperature and ambient temperature in °C, respectively.

Thus, the rate of useful energy extracted by the collector *Qu*, expressed as a rate of extraction under steady state conditions, is proportional to the rate of useful energy absorbed by the collector, less the amount lost by the collector to its surroundings (Smyth et al., 2006). This is expressed in Equation 4 (da Silva and Fernandes, 2010).

$$Q_u = Q_i - Q_o = G\,\tau\alpha\,A - U_L\,A\,(T_c - T_a) \tag{4}$$

Where, *Qu* is useful energy gain in W. The rate of heat extraction from the collector can be measured by means of the amount of heat carried away by the fluid passing through it and is expressed in Equation 5.

$$Q_u = m\,C_p\,(T_o - T_i) \tag{5}$$

Where, *m* is the mass flow rate of the fluid through the collector in kg/s.

In most cases Equation 4 is modified because of the difficulty in defining the collector average temperature. It is easy to define a quantity, which relates to the actual useful energy gain of a collector surface, such as the fluid inlet temperature, T_i. This quantity is known as the collector heat removal factor, F_R (there are actually three types of heat removal factors) for a collector and is shown by Equation 6.

$$F_R = m\,C_p\,(T_o - T_i) / A\,[G\,\tau\alpha - U_L\,(T_i - T_a)] \tag{6}$$

When the whole collector is at the inlet fluid temperature the maximum possible useful energy gain in a solar collector is achieved. The product of the collector heat removal factor, F_R and the maximum possible useful energy gain gives the actual useful energy gain, Q_u, allowing the rewriting of Equation 4. This equation is commonly known as the Hottel–Whillier–Bliss equation, shown in Equation 7 (Duffie and Beckman, 2006).

$$Q_u = A\, F_R\, [G\, (\tau\alpha) - U_L\, (T_i - T_a)] \tag{7}$$

The most useful indicator of a collector's performance is the collector efficiency, η, which can be calculated from Equation 7 as it is defined by the ratio of the useful energy gain, Q_u, to the incident solar energy over a particular time period, expressed in Equation 8.

$$\eta = \int Q_u\, dt \,/\, A \int G\, dt \tag{8}$$

The following equations can be used to define the instantaneous efficiency of the collector.

$$\eta = F_R\, (\tau\alpha) - F_R\, U_L\, (T_i - T_a) \,/\, G \tag{9}$$

$$\eta = m\, C_p\, (T_o - T_i) \,/\, AG \tag{10}$$

These equations form the basis of test standards such as AS/NZS 2535, ISO 9806, ASHRAE 93 and EN 12975. By plotting the collectors efficiency against $(T_i - T_a)/G$, useful information can be obtained. Such as, the slop $(-F_R U_L)$ which represents the rate of heat loss from the collector and the Y-intercept (η_0) being the optical efficiency (though it is actually a combination of the optical absorptance and collector fin efficiency). The parameters acquired from these standardised tests also form the basis for simulation modelling of the performance of SWH systems that use these collectors.

Similar to SWH systems, research on flat-plate collectors has been vast and innumerable. The flat plate collector was initially investigated by Hottel and Woertz (1942), and Bliss (1959), who developed equations which describe the performance of flat plate collectors in terms of its efficiency, as described above. The performance of the collector in terms of design parameters relating to, types of absorber plates were investigated by Mathur et al. (1959) and Patil (1975); number and type of glass covers was studied by Whillier (1963); thickness and type of insulation was studied by Whillier and Saluja (1965); anti-reflective coating on glass cover was studied by Hsieh and Coldewey (1974); heat mirror coating on inner glass as an alternative for selective absorber was investigated by Winegarner (1976); spacing between absorber and inner glass and successive glazings were studied by Nahar and Garg (1980); studies on coatings on absorber plates were taken up by Nahar and Garg (1981).

In summary the majority of works on flat plate collectors have focused on improving heat transfer characteristics through the optimisation of different components, reducing heat losses within different designs and development of new and innovative designs which go hand in hand with the development of technology in the area of solar heating.

1.5.2 Building Integrated Thermal Collectors

One such area has been the emergence of collectors which can be readily integrated into building envelopes or structures for heating applications to address the main problem of architectural uniformity (attractive finish), without adversely affecting performance. These devices have become known as Building Integrated Thermal (BIT) collectors.

Based on this premise a number of studies have investigated innovative solar collector designs that can be integrated directly into the roofing structure without the need for separate roof mounting systems. The results of a large web survey on architectural integration of solar technologies (which was addressed to more than 170 European architects and other building professionals) presented by Probst and Roecker (2007) showed that architectural integration is a major issue in the development and wide spread acceptance of solar thermal technologies. The authors highlighted the need for building integrated collectors to be "conceived as part of a construction system" essentially, solar thermal collectors were to be integrated "into rather than onto" the roofing structure itself as noted by Anderson (2009).

This view was also shared by Medved et al. (2003), who examined an unglazed 'solar thermal' system, essentially a BIT collector, that could be truly integrated into a building, as shown in Figure 5. In their system they utilised standard metal roofing as a BIT collector for the heating needs of an indoor swimming pool. They found that they were able to achieve payback periods of less than 2 years. This translated to a reduction of 75% in the time taken to pay for a glazed system. Furthermore, they report that they were able to achieve efficiencies of over 80% however; these were achieved using collectors with areas of over 200 m^2.

Figure 5: Unglazed integrated solar collector (adapted from Medved, et al., 2003).

Assoa et al. (2007) also presented a concept for a roof integrated water and air heating collector with a high level of integration. They designed a collector in which a water tube was placed in the trough of a troughed-roof system with PV cells added to the ridges, as shown in Figure 6. This type of collector combines preheating of the air and the production of hot water in addition to the electrical function of the solar cells. The authors developed a simplified steady-state two-

dimensional mathematical model of their systems. Using a parametric study (numerically and experimentally) the effect of various factors were investigated, such as the mass flow rate of the water on the solar collectors' thermal performance. They note that the water solar collector mass flow rate has very little influence on the solar air collector behaviour. Furthermore, they theoretically demonstrated that combined efficiencies in excess of 80% could be achieved by their system.

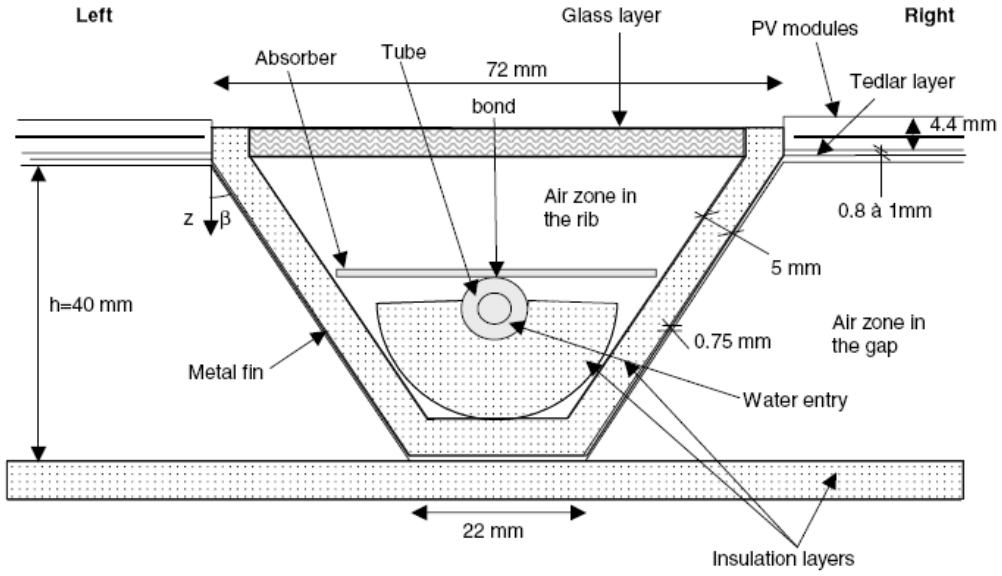

Figure 6: Water and air heating roof integrated collector (adapted from Assoa, et al., 2007).

A similar design to that of Assoa, et al. (2007) was also presented by Anderson et al. (2009). They designed and developed a roof integrated prototype collector that was integrated *into* a standing seam or troughed sheet roof, along with passageways for liquid coolant flow, as shown in Figure 7. Using a modified Hottel–Whillier model they validated results using an outdoor steady-state thermal test rig. Their results concluded that a few key design parameters such as fin efficiency, lamination requirement, as well as thermal conductivity between

the PV module and the supporting structure have significant effects on both the thermal and electrical efficiencies. On the thermal side, they report that they were able to achieve efficiencies of 60% and 30% for glazed and unglazed, respectively. In a concluding remark they suggested that the integration of systems 'into' (rather than 'onto') the roof structure did not need insulation, as the rear air space in the attic can provide a level of insulation equivalent to a highly insulating material.

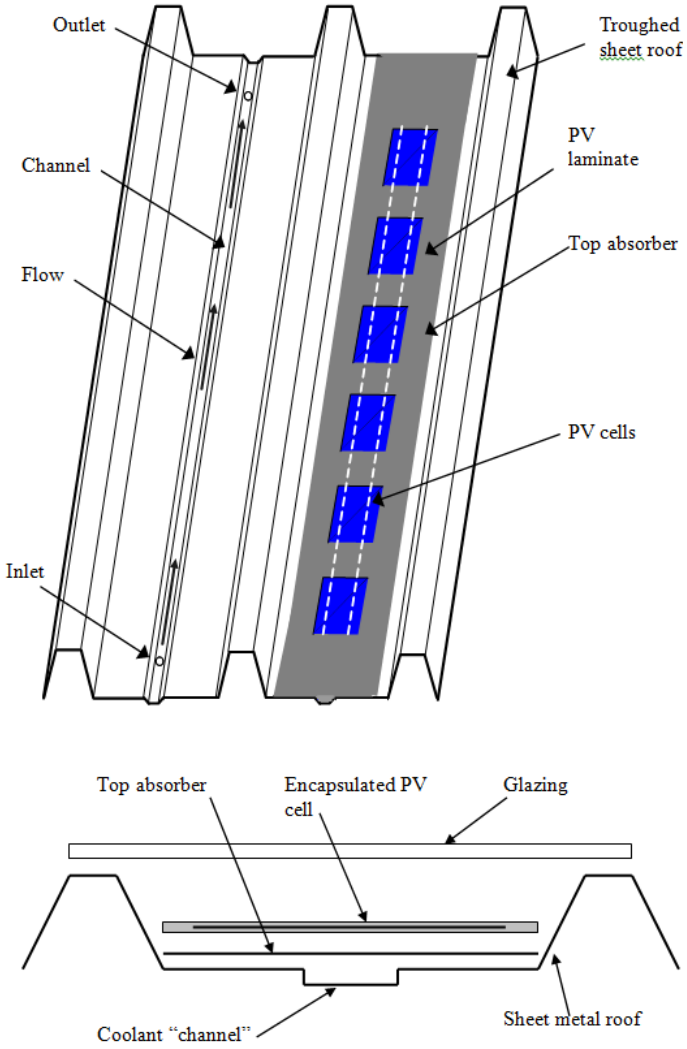

Figure 7: BIPVT collector design (adapted from Anderson, et al., 2009).

Similarly, Wahab et al. (2011) investigated a BIT collector for water heating. They investigated an identical design to that of Anderson, et al. (2009), by using standard long run metal roofing material to produce an integrated (BIT) collector, as shown in Figure 8.

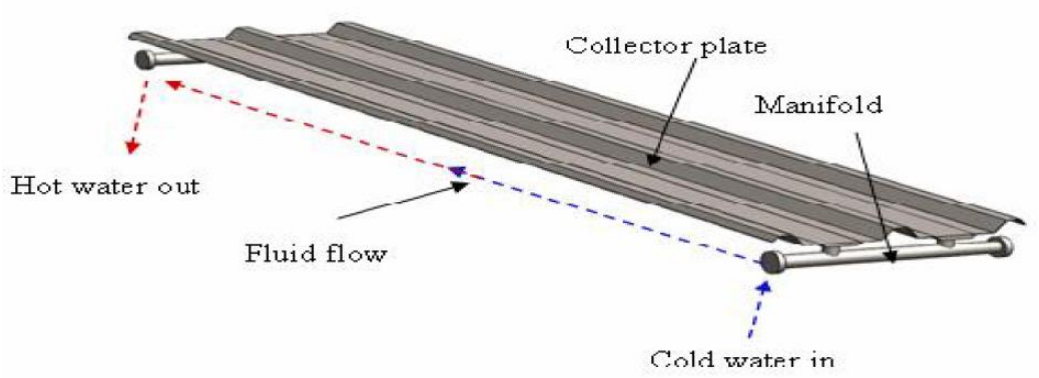

Figure 8: Long run metal roofing BIT collector (adapted from Wahab, et al., 2011).

The authors report that with their collector, they were able to heat an insulated tank (~35 L) of water to approximately 90 °C on a clear sunny day (average solar insolation of 929 W/m^2). Additionally, they report a thermal efficiency of 45 % for the glazed BIT collector and also stated that although the efficiency was relatively low; their system would still be effective as a solar water heater in 'sunny' regions (referring to Australia and New Zealand). Furthermore, they highlight that the possibility of integrating an 'effective' solar hot water system directly into standard roofing material is viable, thus maintaining the aesthetics of the building. Moreover, the main focus of their work was to develop an 'advanced' control strategy for the control of their system, as such, the work from this research was only to serve as a pre-requisite for future work based on control.

1.6 Hypothesis

In light of the review on previous literature, particularly on SWH systems, there is still room for work to be undertaken particularly to 'experimentally' investigate the performance of building integrated SWH systems, specifically in-situ systems with reference to New Zealand conditions. It was observed that the majority of previous research on SWH systems was conducted on commercially packaged systems, which were optimised for flat plate and evacuated tube collectors. Additionally, it has been identified that the majority of solar thermal systems in New Zealand are predominantly water heating systems in the domestic sector (Weiss and Mauthner, 2012).

While previous works on BIT collectors have addressed to some extent the issue of integration and architectural uniformity, there is still room for improvement in terms of achieving both high levels of integration and adequate collector performance. It has been shown that unglazed collectors such as that presented by Medved, et al. (2003) can achieve very high peak efficiencies (>80%), the downside to this is that although it is being used in a low temperature heating application (pool heating) large areas (>200 m^2) are required to achieve effective pool heating. Furthermore, the lack of glazing and insulations makes it unsuitable for domestic water tank heating as it can rarely attain the required temperatures. In an application such as SWH where roofing space is limited, consideration should be made to accommodate for this when designing and developing the collectors.

Although the collectors studied by Assoa, et al. (2007) and Anderson, et al. (2009) have shown good performance, both have incorporated PV cells, which to some extent adversely effects the performance of the overall collector when considering the thermal side. This is because it is desirable to maintain relatively low cell temperatures to achieve optimum cell performance.

One study (Anderson, 2009) did however, investigate the long term performance of their collector (Building integrated photovoltaic/thermal, BIPVT) in a SWH system applicable to New Zealand, but was limited to a simulation analysis using the TRNSYS software and typical meteorological year (TMY) data. The work by Wahab, et al. (2011) provided an indication of how such systems could perform when in a domestic setting, however, the volume of water tested (~35 L) does not represent the volume of consumption of a typical household. Issacs et al. (2010) have found that for showers alone, assuming an average flow rate of 8.4 L/min the average water consumption is 200 L per day.

Additionally, the work (Wahab et. Al, 2011) was only to serve as a prerequisite for their future work on the control of BIPVT systems. To the author's knowledge there is currently little published work that focuses 'specifically' on the performance of 'truly' BIT collectors for use in SWH systems. For this statement conventional flat plate thermal collectors that are flush with the surface of the building façade or roof are not considered 'truly' building integrated.

On this premise it can be said that there still a need for the development of BIT collectors which achieve a high level of integration as well as good collector performance. As a result an experimental investigation of the performance of BIT collectors in an application such as SWH can be undertaken to determine its applicability in a domestic setting, for a country like New Zealand. Therefore the aims of this thesis are to:

- develop a truly integrated BIT collector which addresses architectural uniformity while achieving good collector performance
- investigate the practicality of using the BIT collector in SWH systems for domestic application in New Zealand

1.7 Methodology

Different methodologies exist for the evaluation of the hypothesis described above. It was observed that there is room for improvement in terms of the designing of building integrated collectors to achieve good performance as well as maintaining the building aesthetics. In this case an attempt can be made to design a collector replicating that of a metal long run roof, which is typical of a roofing structure in New Zealand. The reason for this is that such a design could potentially be integrated ‘into rather than onto’ the roofing structure as suggested by Anderson (2009).

Additionally, different methodologies are available for evaluating and characterising the performance of such collectors. It has been observed from previous literature that there is a need for experimental validation of such collectors and perhaps the same evaluation can be applied for a system running with the collector. It has been stated that currently there is no set configuration for BIT water heating systems and therefore its suitability in a domestic setting is yet to be known. Therefore, a combined simulation and experimental approach for such systems can provide a way of assessing and validating its performance.

Based on these premises a methodology was selected to design a BIT to replicate metal long run roofing, experimentally characterise its performance and approach the system performance evaluation using simulation and experimental work.

Chapter 2: Development of a Building Integrated Thermal Collector and Building Integrated Thermal-Solar Water Heating System

2.1 Introduction

The following chapter describes the development of a new design of a BIT collector including the test procedures undertaken to characterise its performance, in terms of efficiency. The subsequent result of this development is that the applicability of the collector for SWH can be investigated. The remaining sections within this chapter describe the development and testing procedure of the BIT-SWH system

2.2 Development of a BIT Collector

The BIT collector used in the SWH system in this study is unique in a number of ways. Similar to the collector design developed by Anderson (2009), this collector can be directly integrated into the roof of a building thus providing a high level of integration. Standing seam and troughed sheet roofs are typically made from aluminium or coated steel, although copper or stainless steel could be used.

The choice of aluminium as the base material for the collector provides high thermal conductivity among other things. Using aluminium, the panel is extruded into a roof-profile shape that gives the roof product stiffness and strength, and when assembled are weather proof. The choice of material provides several benefits. Aluminium is a very versatile material with a range of advantageous properties (Richards, 2009):

- Lightweight - is about one-third the weight of an equal volume of copper, steel or brass. This is especially important as this reduces the load applied on the roofing structure

- Strength - Aluminium can withstand heavy loads and pressure; when alloyed appropriately, its strength approaches that of steel. As a result it has a high strength-to-weight ratio.

- Corrosion resistant - aluminium oxide on the surface of the metal protects it against the corrosive influences of water, salt and other influences.

- Good thermal conductivity - Aluminium distributes heat or cooling energy evenly and quickly.

- Ductile - Aluminium is easy to cold work and fabricate.

- Malleable - The vulnerability of ‘pure’ aluminium to heat and pressure make it ideal for extruding into formed, intricate shapes.

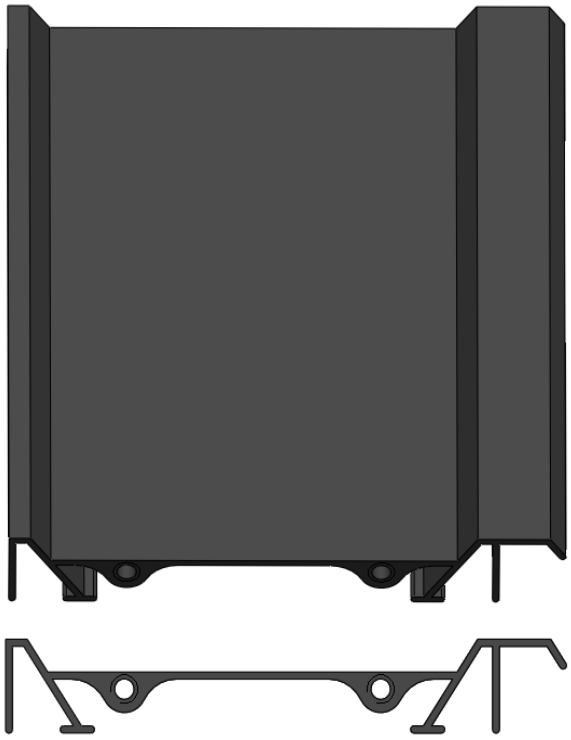

Figure 9: BIT roof panel profile.

Furthermore, the manufacturing process of extruding aluminium is a well-established process (Bauser and Siegert, 2006). One of the many advantages of producing extrusions is the ability to create profiles with intricate shapes and patterns that would unless otherwise be manufactured separately using other manufacturing processes (Bauser and Siegert, 2006). An important component that can be directly produced through extrusion is the channels required for fluid flow, shown in Figure 9; this eliminates the need for further manufacturing, therefore reducing the overall cost of the collector. Another unique feature is the 'interlocking' nature of the extruded panels which provides the opportunity to assemble the collector to a desired geometry, as shown in Figure 10. The aluminium panels were also anodised to increase corrosion resistance (Richards, 2009) and dyed black to give a good surface finish while providing good absorption over the solar radiation spectrum (Anderson, 2009).

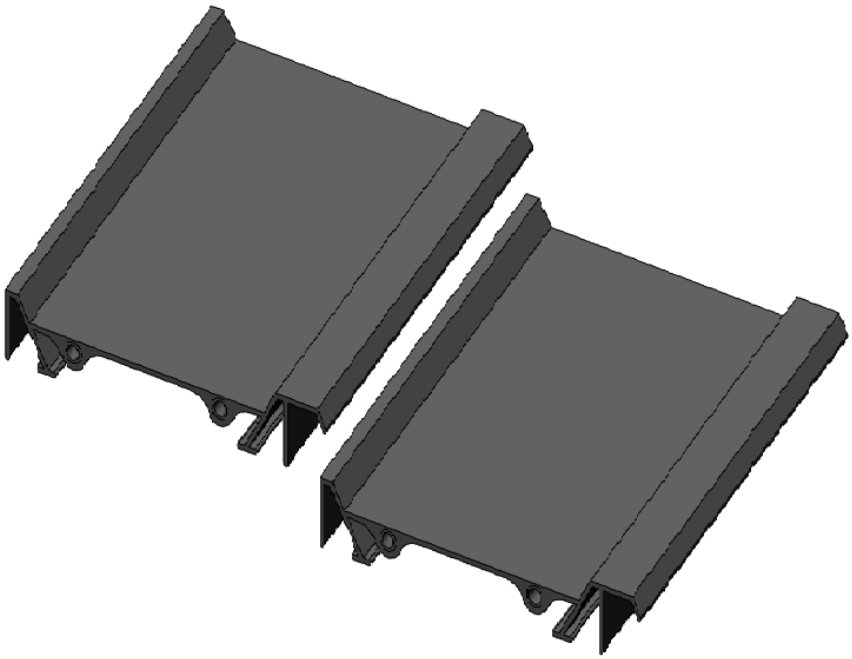

Figure 10: Overlapping panels, creating a BIT collector.

Due to the simple nature of the BIT panels the construction of the collectors was relatively straightforward. The panels were interlocked together to create the desired collector area and mounted onto the testing frame, as shown in Figure 11. The ends of the channels which provide the inlet and outlet (risers) for fluid flow were tapped and fitted with hose fittings so that the manifold could be attached. Based on a numerical analysis specific to this collector design, a manifold to riser pipe ratio of 4:1 was selected as this was shown to be the ideal configuration for achieving a uniform flow distribution throughout the collector (Ghani et al., 2012). The collector risers were linked to the copper manifold (header) using flexible wire (f-w) hose and clamped using standard hose clamps, shown in Figure 12. It should be noted that this method of using f-w hose would not be suitable for a commercial BIT due its unpredictable behaviour under relatively high temperature operation over very long periods, but this was considered adequate for research purposes.

Figure 11: Interlocked panels forming an unglazed collector.

Figure 12: F-w hose clamped onto manifold.

For both the glazed and unglazed BIT collectors the ends of the roof profile were enclosed and the rear surfaces insulated with 50 mm expanded polystyrene insulation, as shown in Figure 13. The glazing used was a low-iron-glass cover placed over the collector to prevent convection losses, side flashings were also used thus forming a glazed building integrated collector with a roof profile, as shown in Figure 14. It should be noted here that the overall collector design was configured to replicate the simplest and most practical configuration of a typical New Zealand household roof, as shown in Figure 15. The design parameters of the BIT collector tested are provided in Appendix A.

Figure 13: End caps on top and bottom of BIT collector with 50 mm polystyrene insulation on underside.

Figure 14: Glazed BIT collector with side flashings and top and bottom end caps.

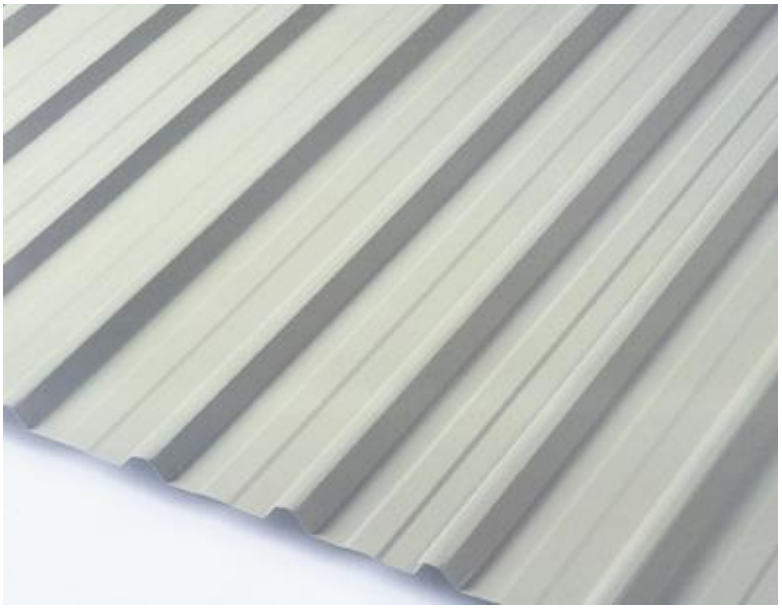

Figure 15: Typical profile of a metal long run roof used in New Zealand.

2.3 Collector Testing Setup

The task of investigating collector performance has been an exercise undertaken for many years. With focus on collector testing in New Zealand conditions, standards such as AS/NZS 2535.1-2007 and ISO 9806-3 can be applied. For this study a steady state outdoor thermal test setup was used, similar to that recommended in AS/NZS 2535.1-2007 and shown in Figure 16 (a schematic diagram is also provided in Appendix B).

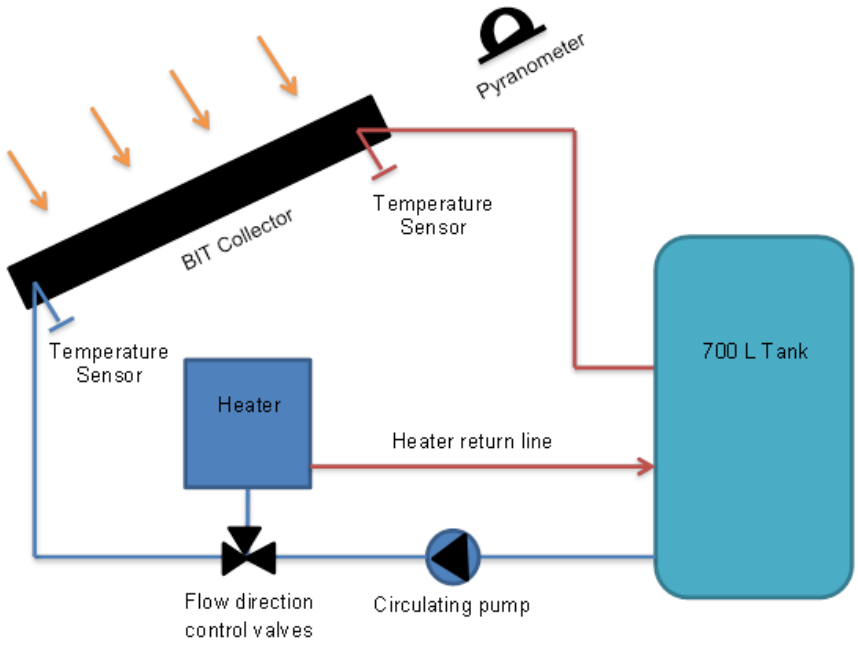

Figure 16: Steady state solar collector testing system.

The main reason for using an outdoor testing system is that the collector performance is characterised based on an actual solar spectrum (Anderson, 2009). This method of testing also provides an insight into conditions expected at a location within New Zealand (Hamilton). Experiments conducted by Anderson (2009) using a similar set-up, showed that the use of outdoor systems is a viable method for solar thermal collector testing. Although there is the possibility of

testing collectors using indoor setups, the need for specialised equipment makes this process financially unviable for this study. Indoors tests are generally conducted using solar simulators, "that is, a source producing radiant energy that has spectral distribution, intensity, uniformity in intensity and direction closely resembling that of solar radiation" (Duffie and Beckman, 2006). The results are also not always comparable to those of outdoor tests because the diffuse-fraction and long wave radiation (which are not the same indoors and outdoors) can affect the relative results of tests (Gillett, 1980). Other studies (refer to Garg et al., 1985, Tiedemann and Maytrott, 1997 and Adelhelm and Berger, 2003) have also found that using indoor solar simulators showed either poor replication of the solar spectrum or non-uniform illumination, further supporting the use of an outdoor system.

To obtain accurate test results the test location is important, therefore an unimpeded north facing test location at The University of Waikato's Aquatic Research Centre was chosen, Figure 17 (left). To quantify the performance of the collector it was necessary to measure the global incident solar radiation at the test location. The measurement of the incoming radiation was made using a WMO First Class pyranometer which had been recently calibrated, mounted in-line with the collector at an angle of 38 °C which is equal to the local latitude, shown in Figure 17 (right). A cup anemometer which is used to monitor wind speed in the test area was mounted adjacent to the test stand for the collector, shown in Figure 17 (right).

Figure 17: Left-unimpeded test location at the Aquatic Centre, right-pyranometer and cup anemometer.

K-type thermocouples were used to measure the inlet and outlet temperatures to the collector and the local ambient air temperature, Figure 18 (left). In addition to the measurement apparatus, an instantaneous gas water heater with an inbuilt temperature controller was also mounted on the inlet side of a 700 litre tank, as shown in Figure 18 (right). The outlets from the collector and the water heater was returned to the water tank, as shown in Figure 19, the reason for this was to provide a means of controlling the inlet water temperature which for fills the requirements for collector testing as set out in the AS/NZ 2535 standard.

Figure 18: Left-thermocouples mounted to inlet and outlet, right-instantaneous water heater and water tank.

Figure 19: Fluid channels to and from the collector and water heater.

The flow of water through the collector was set at a constant rate by manually adjusting the valves at the inlet to the collector, shown in Figure 19. The flow rate values were measured by manually measuring the time taken for a known mass to pass through the collector.

The testing of the BIT collectors was conducted in accordance with AS/NZS 2535.1-2007. This standard specifies a test method to determine the thermal efficiency of solar collectors. A prerequisite to accurately determining the performance of the collector is to conduct a number of outdoor tests under a range of ambient conditions. In this study both a glazed and unglazed BIT collector were tested.

To collect all the data needed for analysis, a data acquisition (DAQ) program was developed using National Instruments (NI) systems design software, labVIEW, shown in Figure 20. This program allowed the user to control all aspects of data logging including, save file locations, tested collector area and flow rate and user specified logging intervals.

For each test the temperatures, global radiation and wind speed were data-logged at 20 second intervals. At the beginning of each test period the collector was pre-run for 15 minutes so as to reach a quasi-steady state. In analysing the data, only 5 minute periods when the average global radiation exceeded 800W/m^2 and did not vary by more than 50W/m^2, the ambient temperature did not vary by more than

1K and the inlet temperature did not vary by more than 0.1K were taken to be steady-state.

Additionally, any data points that satisfied these criteria but were more than 30 degrees either side of solar noon were also eliminated due to the possibility of including incident angle modifier terms.

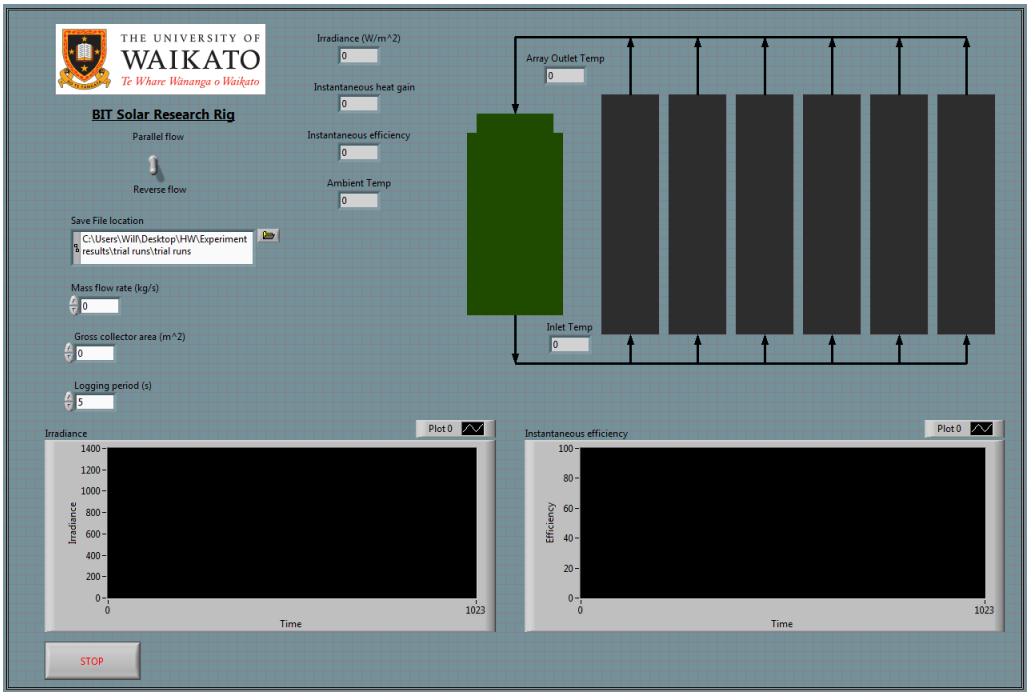

Figure 20: Front panel of the labVIEW DAQ program.

2.4 Development of a BIT-SWH System

With the development of the BIT collector now complete, its applicability for SWH was investigated. There are many different SWH system configurations, the most common water heating systems is however well documented and reviewed elsewhere (Duffie and Beckman, 2006). In this study the SWH system that was chosen is based on the forced circulation (indirect or close looped, drain-back) system configuration. An overview of the system is shown if Figure 21. All the major components of the system shall be illustrated and discussed separately within this section (a schematic is provided in Appendix B).

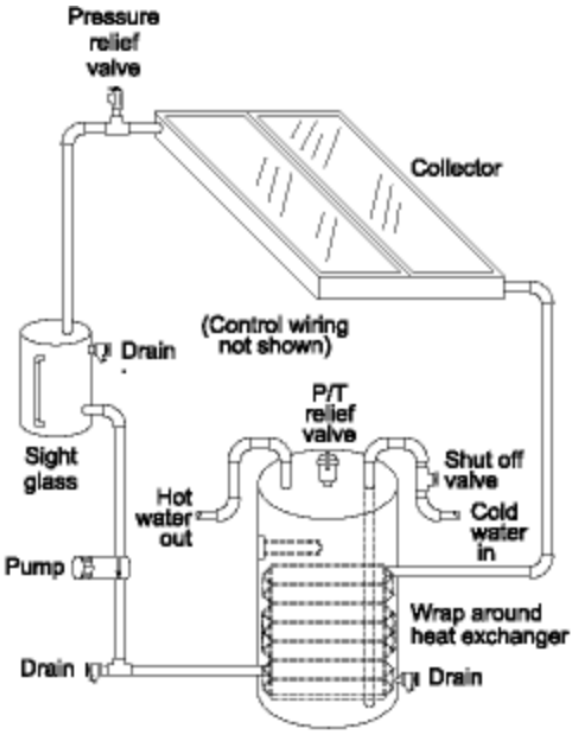

Figure 21: A typical SWH forced circulation indirect (or closed loop), drain-back system (adapted from Harrison et al., 1985).

The difficulty with choosing an appropriate system configuration for this specific collector lies in the fact that current commercially available systems are packaged systems; which are optimised for use with traditional collectors (flat plate or evacuated tube). Since the design of the BIT collector closes matches that of a flat plate collector it was decided that the forced circulation configuration would be used. It was also chosen because it is a good representation of a typical SWH system in single family households in New Zealand (Weiss and Mauthner, 2012). A study report by Pollard and Zhao (2008) surveyed a total of 39 SWH (and HPWH) systems in different locations within New Zealand. Of this, a total of 25 were pumped systems using either a flat plate or evacuated tube collector, as shown in Figure 22, thus supporting the use of this system configuration.

City/technology	Evacuated tube pumped	Flat pumped	Flat thermosiphon	Heat pump
Auckland	3	5	1	3
Wellington	3	3	3	-
Christchurch	3	3	3	-
Dunedin	4	1	3	1

Figure 22: Surveyed houses by each technology defined by region (adapted from Pollard and Zhao, 2008)

As mentioned in the above section the collector used is unique, therefore the SWH system investigated in this study is unique. It utilises the BIT collector connected to a forced circulation drain-back configuration providing a novel BIT-SWH system. Another reason for choosing the forced circulation drain-back system is, pragmatically, it is a fail-safe method of ensuring that the collectors and collector loop piping never freeze. This is a major feature of the drain-back system, providing freeze protection when the system is in drain mode. Water in the collectors and exposed piping drains into the insulated drain-back tank each time

the pump shuts off. Since the collector is already at a slight tilt to receive incident radiation, this allows the collector to be completely drained. A sight glass attached to the drain-back tank shows when the reservoir tank is full and the collector has been drained.

2.4.1 Collector

As stated previously, a novel BIT collector was developed, constructed and experiments conducted to characterise its efficiency. The construction of the BIT collector for the SWH system was similar to the collector tested; however the area was modified to give a gross collector area of 6 m^2 compared with 2.4 m^2 for the tested collector. All others aspects such as, collector enclosement, insulation, fittings and glazing were identical to the tested collector. The BIT collector used for SWH is shown in figure 23.

Figure 23: Glazed BIT collector used in SWH system.

2.4.2 Drain-back and Storage Tank

Drain-back Tank

Within a drain-back configuration, two loops are present, the collector loop (containing the drain back tank) and the load supply loop (storage tank). The collector loop as the name suggests, deals with the flow of fluid from the drain-back tank through the heat exchanger to the collector and back, as shown in Figure 24. In this particular system, water was chosen as the collector loop heat transfer medium. Other options for fluid mediums include different types of glycol/water mixtures which have anti-freeze properties; however certain mixtures deteriorate over time producing acids that can erode away piping (Harrison, et al., 1985). The drain-back tank used in the system is shown in Figure 24.

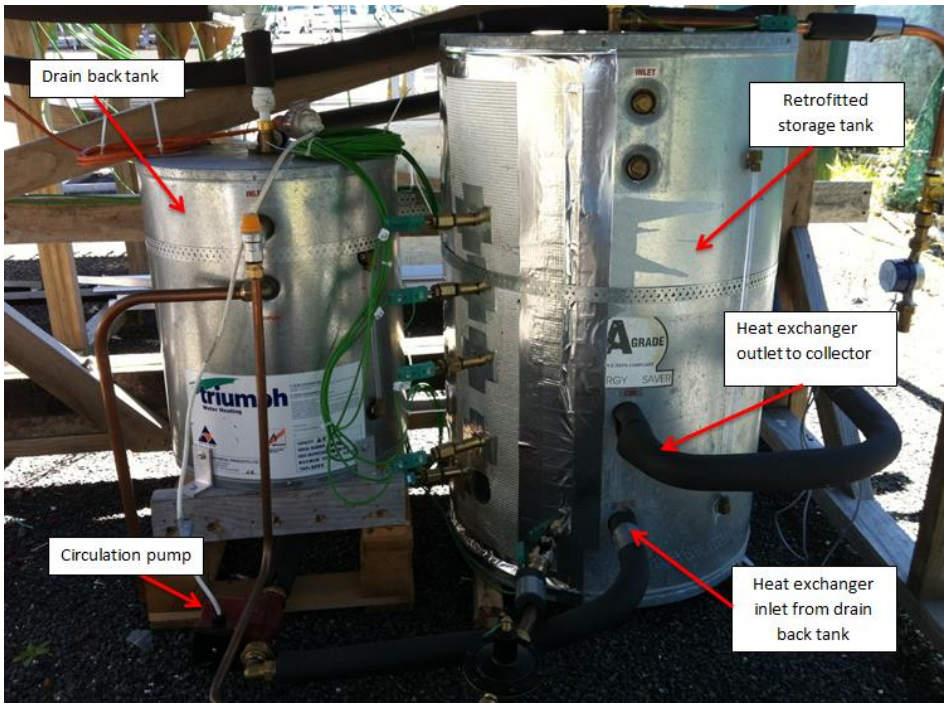

Figure 24: Drain-back tank and inlet and outlet to heat exchanger.

Another feature of the drain-back tank is the column of air within the tank. Although, the primary function of the drain-back tank is to store the fluid that has 'drained back' from the collector and piping when the pump has switched off, it provides another advantageous function. This occurs when the pump is switched back on and fluid is pumped throughout the system, all the air trapped in the system is pushed out and back into the drain-back tank where the column of air exists. Ideally, an air bleed valve would be present at the highest point of inclination to allow trapped air to escape, however this method proved effective in achieving the same result.

One major issue this configuration also overcomes is heat loss during the night time period caused by back or reverse circulation (thermosiphon process). During the night when sufficient solar gains isn't available to heat the water using the collector, the circulation pump isn't operating. The assumption here is that the collector loop then becomes redundant. However, it was observed (Pollard and Zhao, 2008) that during the night, hot water from the top of the hot water cylinder travelled upwards to the collector where it lost heat to the environment, as shown in Figure 25. With a drain back configuration, during the night when the pump has shut off all the water in the collector loop is drained, eliminating the possibility of back circulation occurring.

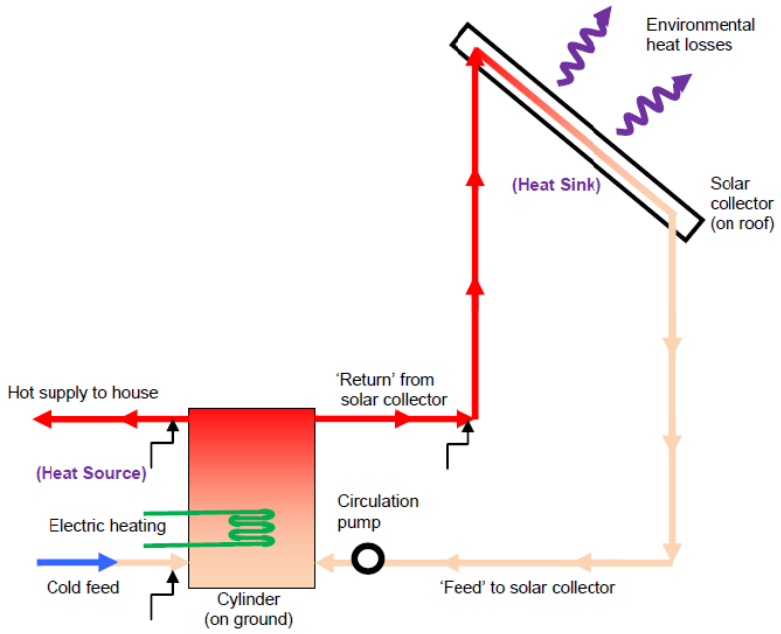

Figure 25: Heat loss caused by night-time back circulation (adapted from Pollard and Zhao, 2008)

Storage Tank

With this particular system, the heat exchanger for the collector loop is within the storage tank. The heat exchanger is commonly in the drain-back tank which is then connected to the storage tank. The reason for this unusual configuration is because the storage tank is actually a drain-back tank that was retrofitted and used as the storage tank. The advantage of this is that sensor pockets could be mounted to the tank to provide an accurate measurement of the level of stratification within the storage tank, as shown in Figure 26. A 2 kW in-tank immersion element was also fitted to the bottom of the tank to provide the supplementary heating generally required in SWH systems. It should be noted here that although supplementary heating is essential in commercial systems (including safety reasons such as legionella control), it is of more interest to this study to observe the performance of the solar only part of the system, therefore the heating component of the storage tank was disregarded. A pressure relief vent was also

retrofitted to the storage tank for safety reasons. The pressurisation of the storage tank also meant that only a single pump was needed, because when the solenoid valve is opened water under pressure in the tank is forced out due to the pressure caused by the flow of water from the inlet.

Other components included the circulating pump (refer to Figure 24) for the collector loop and solenoid valve which simulated the load drawn from the storage tank by the household, shown in Figure 26. It should be noted that a tempering valve is commonly present on the inlet side of the storage tank to control the temperature of the outlet to the household; this aspect was not considered as it would have no effect on the thermal performance of the BIT-SWH system.

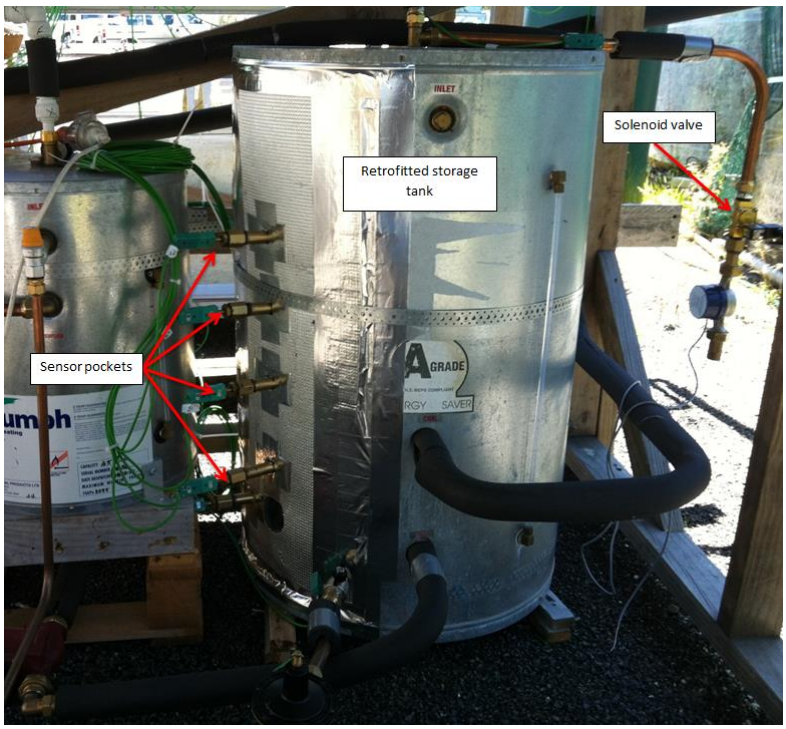

Figure 26: Retrofitted storage tank and sensor pockets.

2.4.3 Control System

Similar to the DAQ program used during the testing of the BIT collector, the program used for the control of the SWH system was developed using the NI labVIEW software. As addressed in an earlier chapter, numerous control strategies are available for the control of SWH systems. The program developed for this study can be separated into 3 sections as listed, pump control, load draw off simulation and data storage (or acquisition). The program front panel is shown in Figure 27.

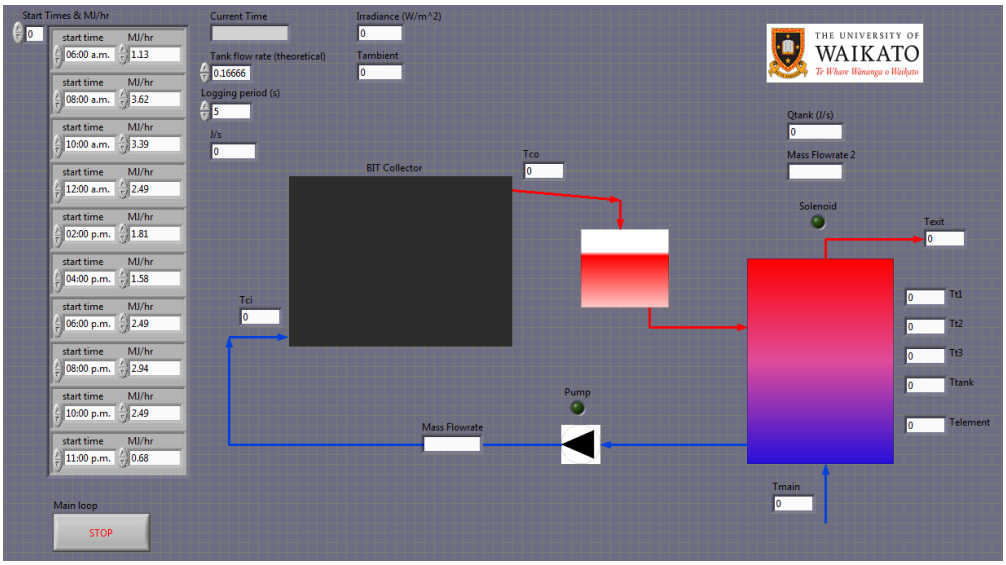

Figure 27: Front panel for SWH system program.

Pump Control

The control of the circulation pump was based on the temperature differential principle. The differential controller (or algorithm) uses the temperature differences between the water leaving the solar collector (in the collector loop) and the coldest water in the storage tank, in this study the collector outlet temperature (T_{co}) and the temperature reading in the cold region of the storage

tank (T_{tank}) were used to represent these parameters, respectively. When the temperature at the outlet of the collector was about eight to ten degrees warmer than the water in the tank, a signal was sent by the controller to turn the pump on. When the temperature difference dropped to about four degrees, the pump was turned off. In this way, the water always gained heat from the collector when the pump was operating. A safety precaution that was built into the control strategy was for the case when the water at the top of the tank (T_{t1}), was greater than 90 °C. If such an incident were to occur a signal was sent by the controller to switch the pump off to avoid overheating.

.

Load Draw-off Simulation

One of the challenges encountered during the development of the SWH system was how it would be run to replicate its operation in a normal day to day application. From a practical point of view and due to the relatively remote nature of the location, it was decided that the daily water draw off profile or load consumption pattern was to be simulated. This was carried out using a standardised load profile which simulated the use of the system in a single family household in the New Zealand climate zone. As such a control strategy was developed based on the standardised load profile provided by the AS/NZS 4234 standard, to control the periods were load was being drawn from the system. This was achieved by fitting a solenoid valve to the outlet of the storage tank and then signals were sent by the controller to open and close the valve when draw off was required. The load profile provided by the AS/NZS 4234 standard is discussed in detail in the proceeding section (System testing setup).

Data Acquisition

Data acquisition was achieved much the same as for the collector testing. The local time and the time when signals were sent to the pump and solenoid valve were gathered and stored in text based files. Logging intervals were also specified by the user and data including, ambient temperature and irradiance as well as collector and storage tank temperature readings were recorded and stored for later analysis.

The uniqueness of the BIT-SWH system provided a number of challenges during the development and construction stage. Components such as the heating element, tempering valve and flow metre on the outlet of the storage tank all provided issues which were disregarded. The heating element was not needed as an investigation of the solar only section of the system was desirable. The tempering valve would not affect the performance of the system aside from controlling the outlet temperature of the storage tank. An estimated flow-rate was obtained by using manual measurements and this was considered adequate. A list of the components and parameters used in the BIT-SWH system tested is provided in Appendix A.

2.5 System Testing Setup

For this study an experimental outdoor test setup similar to that used by Wahab, et al. (2011) was chosen. The reason for this is because it replicates a SWH system in a typical single family, as shown in Figure 28. An important requirement during the development of the experimental rig was that it had to be flexible

enough to accommodate for future work, aside from this study. This is because different research projects were also being conducted at the Aquatic centre. Therefore, the construction of the SWH testing set-up was kept as simple as possible, while achieving a good representative of a SWH system. The temperature sensors for the storage tank were labelled as follows, beginning from the sensor near the top: T_{t1}, T_{t2}, T_{t3}, T_{tank} and $T_{element}$.

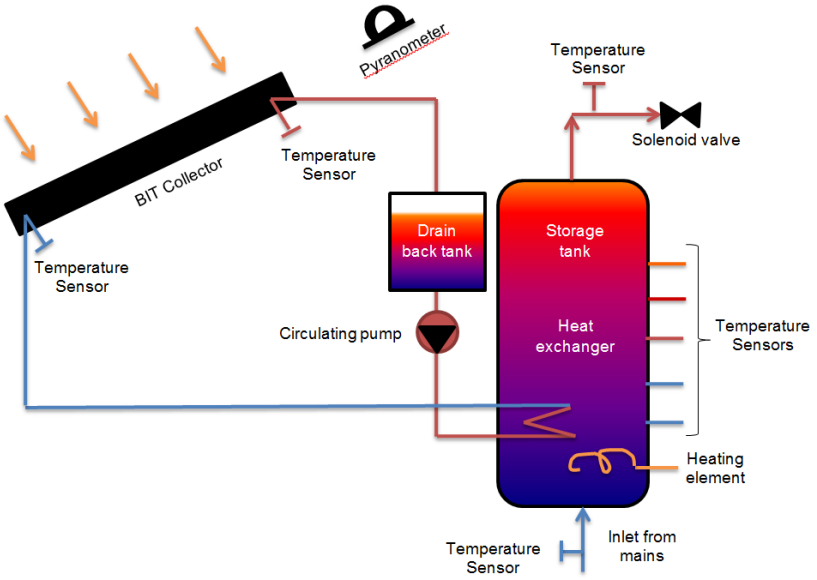

Figure 28: Experimental set-up of SWH system.

To quantify the performance of the system it was necessary to measure the global incident solar radiation at the test location. The measurement of the incoming radiation was made using the same calibrated WMO First Class pyranometer, used for collector testing however the inclination was modified to watch the BIT-SWH at an angle of 5 °.

Similarly, K-type thermocouples were used to measure the ambient, inlet and outlet temperatures to the collector and the storage tank temperatures. Because of the issues encountered with the flow meter on the outlet of the storage tank, an estimated value of 10 L/min was used. This flow value was obtained by manually measuring the time taken for a known mass to exit the storage tank within a given period. There will however, be differences in the actual experimental value caused by pressure drops if say a tempering valve was present on the inlet. For the flow rate through the collector a value of 18 L/min was used as this was pre-determined by the setting on the pump.

As stated earlier, the load profile of the system was achieved by simulating a standardised load profile as described in AS/NZS 4234:2008, this is shown in Figure 29. The hourly load is measured in MJ/hr.

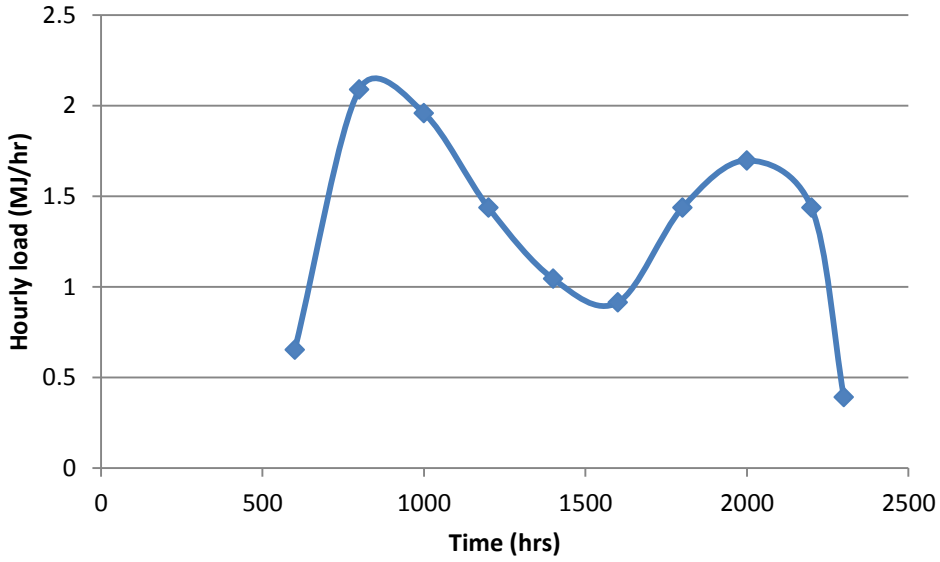

Figure 29: Standardised load profile from AS/NZS 4234:2008.

Chapter 3: Experimental Performance of BIT Collector and SWH System

3.1 Introduction

With the task of constructing the collector testing and BIT-SWH testing systems complete, experiments could be conducted to evaluate their performances. The following chapter describes the results obtained from experimentation and derivation of data into meaningful results. Each section regarding experimentation discusses the findings observed from the results, concluding with a summary at the end of the chapter.

3.2 Experimental Performance of BIT Collector

When analysing the collectors, the instantaneous collector efficiency can be determined directly from the experimental results, as it is defined simply as the ratio of heat transfer in the collector (Equation 11) to the product of the collector area and the global solar irradiance, as shown in Equation 12 (energy out/energy in). These are the Hottel-Whillier equations described above, the efficiency of the collector was determined using the gross collector area (A_G).

$$Q_{collector} = m\ Cp\ (T_{co} - T_{ci}) \tag{11}$$

$$\eta_G = Q_{collector} / G\ A_G \tag{12}$$

However, further analysis of the raw data is required to determine the efficiency equation of the BIT collectors. From the experimental data, the efficiency of the

BIT collector for ‘all’ conditions can be represented by a linear equation of the form shown in Equation13.

$$\eta = \eta_0 - a_1 \, (T_{ci} - T_a / G) \tag{13}$$

To determine the efficiency of the BIT collectors, experimental data was analysed for when the collector met the conditions for steady state operation. The instantaneous heat gain and collector efficiency were also calculated for both unglazed and glazed collectors. Details of the values used are provided in Appendix C.

From the experimental data, it was possible to derive the performance of the collectors using a linear least squares regression analysis. As a result two equations are produced that describe the unglazed and glazed collector efficiencies, as shown in Equation 14 and 15, respectively.

$$\eta = 0.39 - 13.5 \, (T_{ci} - T_a / G) \tag{14}$$

$$\eta = 0.75 - 23.2 \, (T_{ci} - T_a / G) \tag{15}$$

A graphical representation of the equations describing the collector efficiencies is shown below in Figure 30 and Figure 31 for unglazed and glazed, respectively. A couple of important parameters that can be deduced from these figures are the optical efficiencies of the collectors (η_0) which is the y-intercept of the graphs.

This is when the collector inlet temperature is at equilibrium with the surrounding conditions (for the case where $T_{ci} - T_a = 0$). The other being the rate of heat loss from the collector ($-F_R U_L$), represented by the slope of the linear relationship. From these graphs it can be seen that as the difference in temperature between the collector inlet and the ambient increases, at constant radiation intensity, there is a decrease in collector efficiency. When comparing the optical efficiency of the collectors it is observed that the glazed collector is much higher (75%) compared to the unglazed (39%). Additionally, it is interesting to note that the glazed BIT collector has a much higher rate of heat loss when compared with the unglazed collector. It has almost doubled with a value of -23.3 compared to -13.5 for the unglazed.

To gain a better understanding of these values, a comparison can be made. As stated earlier, the collector design for this study was based on a similar design developed by Anderson (2009). It has also been stated that the collector developed by Anderson (2009) has good performance. Therefore, a comparison of the efficiency curves for the two collector designs is a good benchmark of a well performing integrated collector. The efficiency curves for the unglazed and glazed BIPVT collectors developed by Anderson (2009) are shown in Figure 32 and Figure 33, respectively.

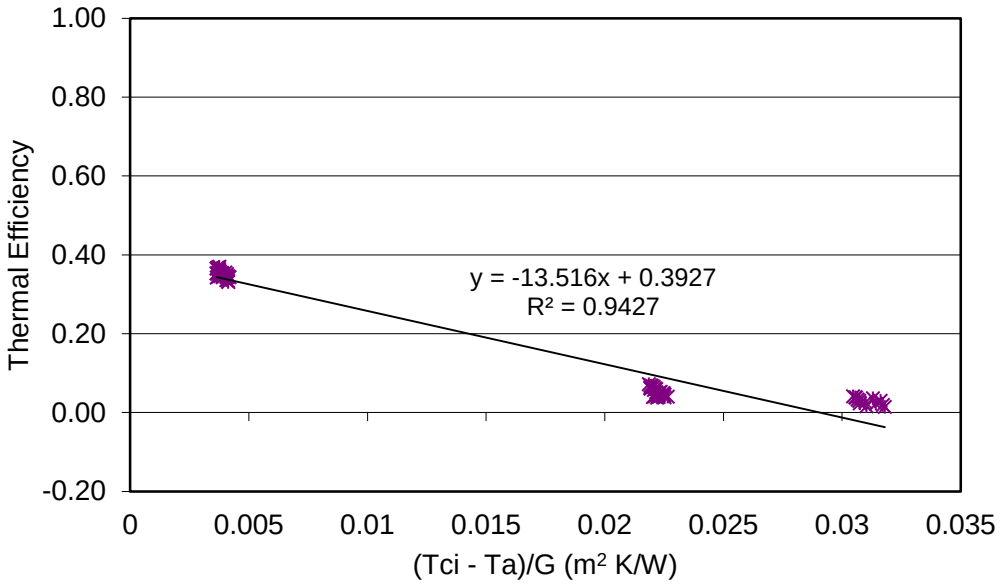

Figure 30: Thermal efficiency of unglazed BIT collector.

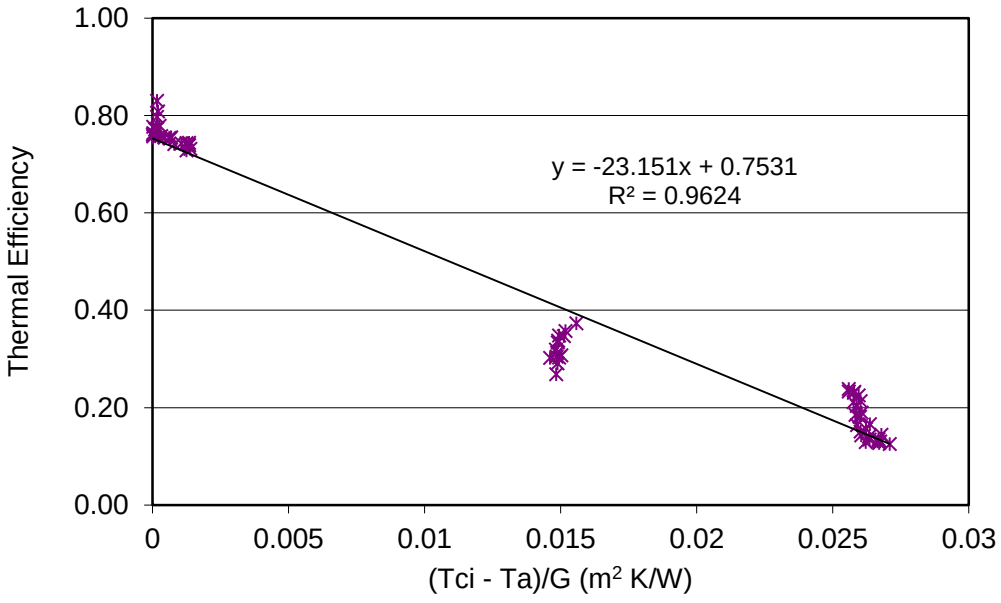

Figure 31: Thermal efficiency of glazed BIT collector.

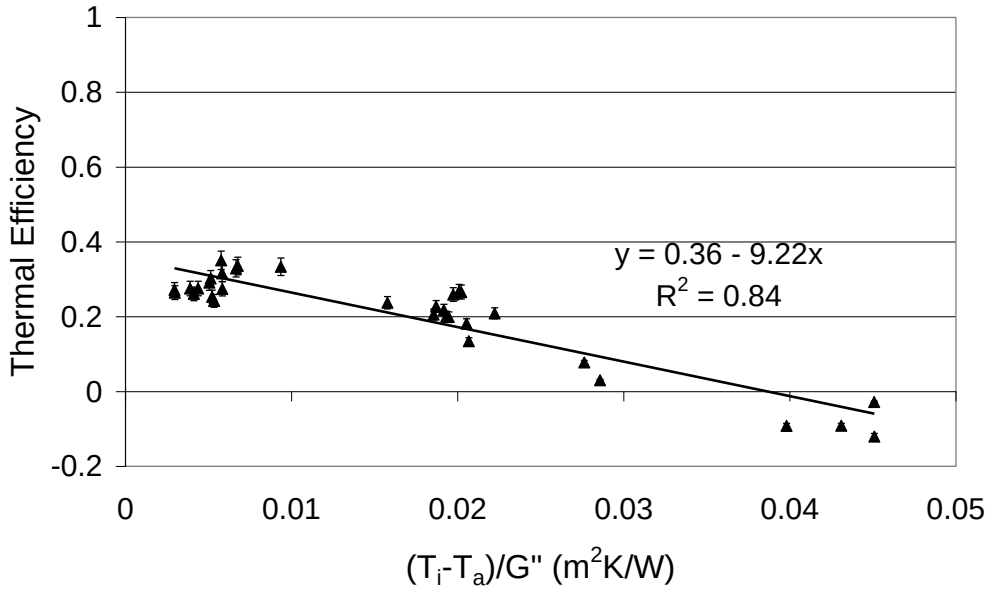

Figure 32: Thermal efficiency of prototype unglazed BIPVT collector (adapted from Anderson, 2009).

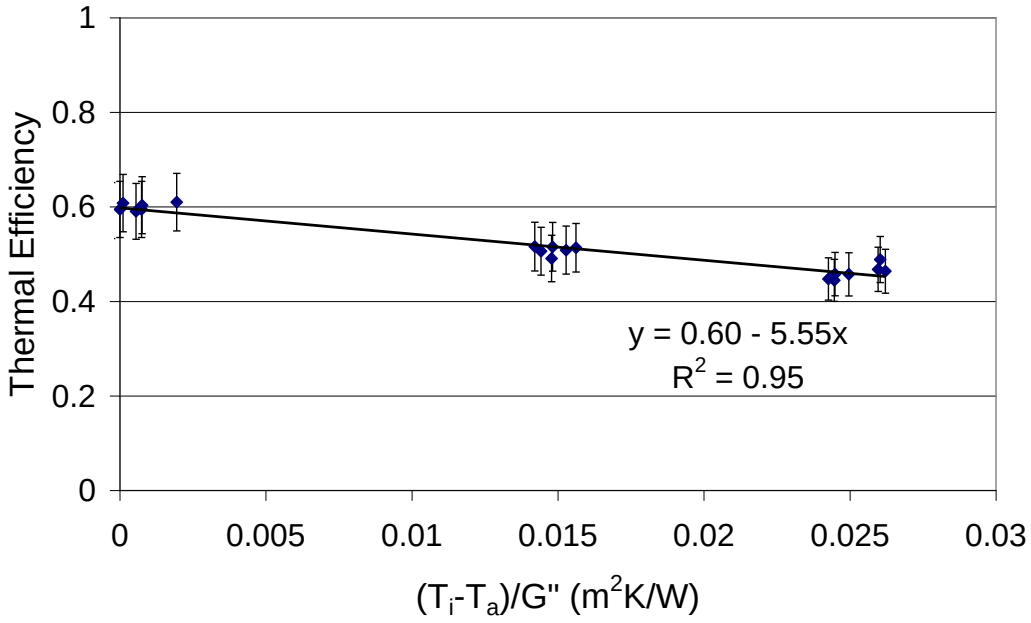

Figure 33: Thermal efficiency of prototype glazed BIPVT collector (adapted from Anderson, 2009).

If we first observe the un-glazed collectors, the results show good agreement in terms of the optical efficiency and rate of heat loss. However, there is a slight increase in both the optical efficiency and slope for the BIT collector. This is directly related to the presence of the PV cells within Anderson's (2009) design; the optical properties of silicon means that the PV cells tend to reflect a large portion of the solar spectrum (Green and Keevers, 1995).

To gain a better understanding of the results obtained for the glazed collector, it is observed from a theoretical perspective, the collector performance and thus efficiency is largely dependent on the collectors heat gain, shown in Equation 16.

$$Q_u = A\, F_R\, [G\, (\tau\alpha) - U_L\, (T_i - T_a)] \tag{16}$$

The underlying parameter that affects the heat gain can be better understood by observing Equation 17. The heat removal factor, F_R, defines the actual useful energy that is gained by the collector compared to the useful gain if the whole collector was at the fluid inlet temperature (the implication of this is that the collector is performing at its thermodynamic optimum, where the temperature difference between the absorber and the environment is at its minimum).

$$F_R = m\, C_p / A\, U_L\, [1 - exp\, (A\, U_L\, F' / m\, C_p)] \tag{17}$$

The important parameter for determining the heat removal factor of the collector is the collector efficiency factor, *F'*, which is derived from Equation 18.

$$F' = [1/U_L] / W [1 / UL (D + (W-D) F) + 1 / C_b + 1 / \pi D_i h_{fi}] \quad (18)$$

The significance of the collector efficiency factor is, it terms of the physical construction of a collector, the denominator describes the thermal resistance between the working fluid and the ambient air, while the numerator describes the thermal resistance between the collector surface (or absorber) and the ambient air.

The key parameters related to the collector efficiency factor are bond conductance, C_b, heat transfer inside the tube or flow channels due to flow variation, h_{fi} and the fin efficiency, F. All three parameters are to some extent dependent on temperature, however for most collectors the fin efficiency is the most important variable in determining the collector efficiency factor.

This can be better understood by looking at the fin efficiency equation, shown in Equation 19. The fin efficiency in relation to the fluid flow channels is defined simply as 'the ratio of the rate of heat flow through the real fin to the rate of heat flow through a fin of infinite thermal conductivity, that is, a fin at uniform temperature (Goswami et al., 2000).'

$$F = [\tanh M (l'-D)/2] / [M (l'-D)/2] \quad (19)$$

Where M can be found from Equation 20 and l' and D representing physical dimensions of the collector plate shown in Figure 34.

$$M = (U_L / k_A t)^{1/2} \quad (20)$$

In the above equation, $U_{L,}$ is the overall heat loss coefficient or conductance of the collector (it is a summation of the sides or edge + top + bottom heat loss coefficients), k_A is the thermal conductivity of the collector absorber material and t is the absorber thickness (refer to Figure 34).

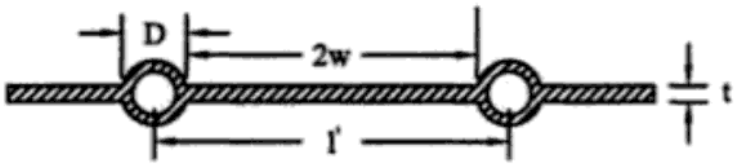

Figure 34: Sketch showing dimension of plate and fluid channels (adapted from Goswami, et al., 2000).

Alternatively, the fin efficiency can be obtained from a plot of fin efficiency against the dimensionless parameter $M (W-D / 2)$, as shown in Figure 35.

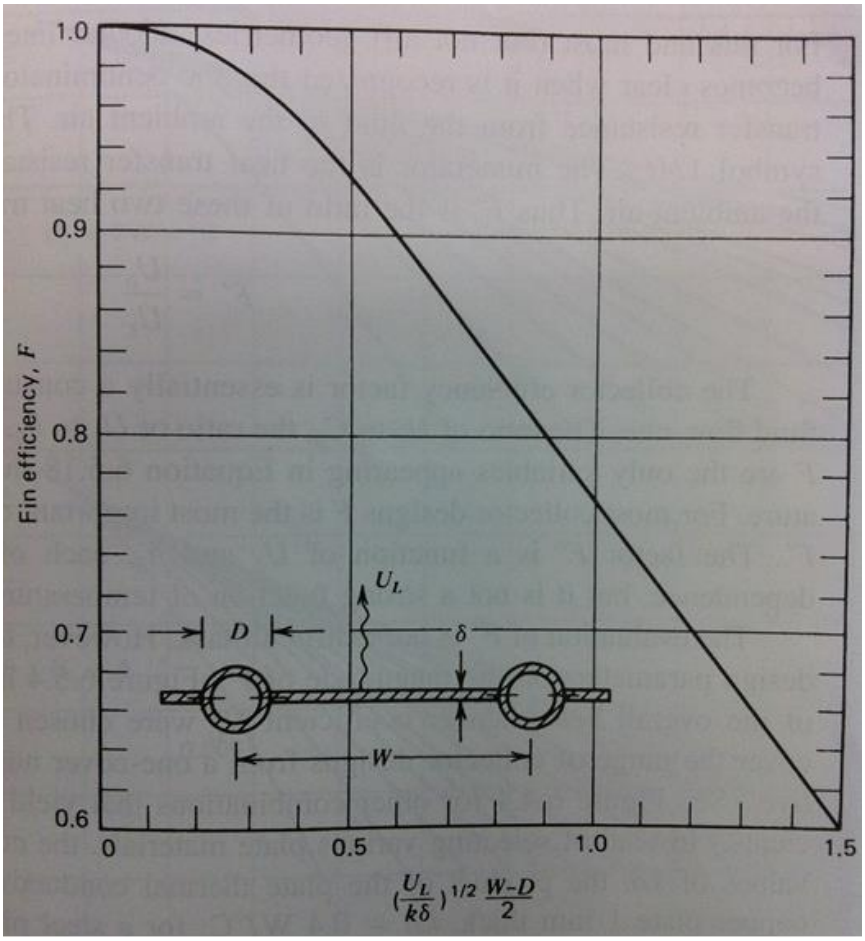

Figure 35: Fin efficiency for tube-and-sheet solar collectors (adapted from Duffie and Beckman, 2006).

It is evident from Equation 20 and Figure 35 that the fin efficiency of the collector is largely dependent on two factors, the total heat loss and the thermal conductivity of the absorber material. The relation this has to collector performance is through the collector efficiency factor and subsequently the heat removal factor. On a side note this process is typically used to determine the theoretical thermal efficiencies of sheet-and-tube designs, such as the BIT and BIPVT. The calculation of theoretical thermal efficiencies was an exercise disregarded as it was considered, outside of the scope of this study.

If a comparison of the physical construction of the BIT and BIPVT collectors is made, it is evident that the BIT collector should, in theory at least, have a higher heat gain, due to higher fin efficiencies. This is a result of increasing the absorber thermal conductivity from 50 W/m K (coloured steel) to over 200 W/m K (aluminium). The implication of this is that the collector efficiency factor and therefore heat removal factor, increases thus increasing the heat gain and thermal efficiency of the BIT compared to the BIPVT. This has been proven experimentally, shown by the increase of the maximum thermal efficiency from 60% for the BIPVT to 75 % for the BIT collector. This highlights the advantages of using a collector base material with higher thermal conductivity.

In terms of the high heat loss observed for the BIT collector reference can be made again to the fin efficiency, and more specifically the overall heat loss of the collector, U_L. As stated earlier it is the summation of the edge, top and bottom losses. It should be noted here that, that the top losses for both collectors was assumed to be similar due to both collectors using low iron glazing and black absorbers.

For the bottom losses it was first observed that there were differences in insulation, the BIT collector used expanded polystyrene which has a typical thermal conductivity of 0.037 W/mK (Bondor, 2013) compared with 0.045 W/mK for the mineral fibre insulation used by Anderson (2009). Although the thermal conductivity values are similar, the thickness of the applied insulation also has an impact on thermal losses or the thermal resistance of the system (Harley, 2002).

This would explain why higher heat loss is observed for the BIT, because a thickness of 50 mm was used for the BIT design compared with 100 mm, which means that the thermal resistance has effectively doubled for the BIPVT. Additionally side or edge insulation was applied to the BIPVT collector, where only side flashings represented by 2 mm thick aluminium and end caps made from standard roofing iron were used for the BIT, shown in Figure 36.

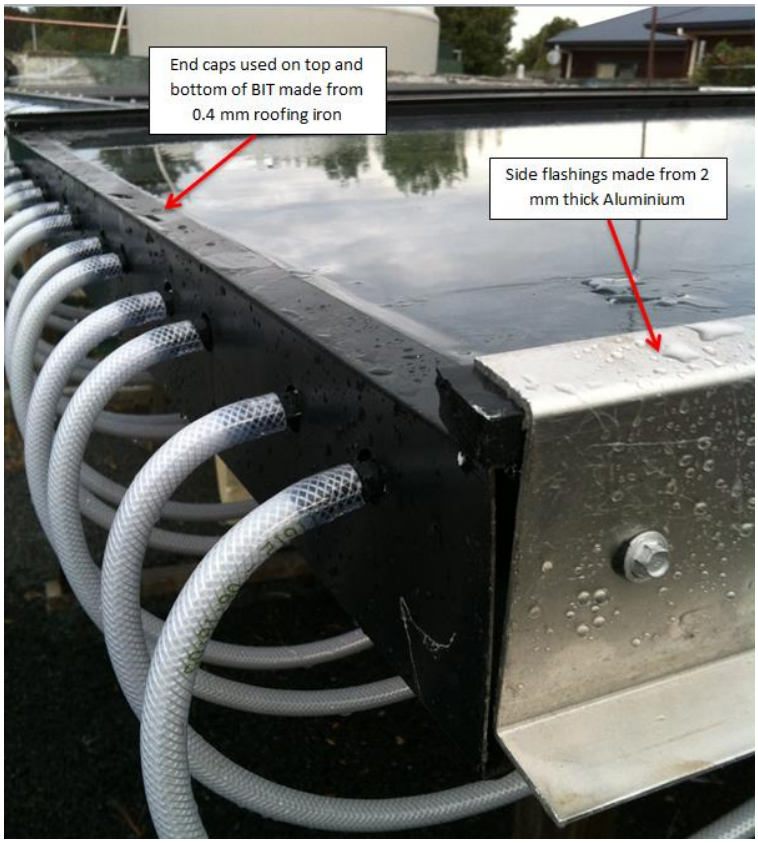

Figure 36: Side flashings and top/bottom end caps.

The significance of the insulation can be better understood from an inspection of Equation 21. The R-value (Km^2/W) in the equation is a measure of the thermal resistance of an insulating material, a term commonly used in the building and construction industry to characterise insulation performance (Bynum, 2001).

$$R = L_{in} / k_{in} \tag{21}$$

Where L is the thickness of the insulation material in m and k_{in} is the corresponding thermal conductivity in W/m K.

From this equation it can be seen that as the thickness of the insulation increases the thermal resistance also increases. This is assuming that thermal conductivity remains constant throughout the insulation material. From the equation the effective R-value (thermal resistance) of the BIT is 1.35 Km^2/W compared with 2.22 Km^2/W for the BIPVT, resulting in higher heat loss from the BIT. Although the side flashings and end caps isolated the collector from the possibility of heat losses which can occur through high radiative heat losses from the collector to the sky (due to the high emissivity of the collector and low sky temperature) and convective heat losses by natural convection and wind induced forced convection (Anderson, 2004), the lack of insulation on the sides has consequently contributed to high heat loss due to conduction between the collector absorber and aluminium flashing of the BIT.

Additionally, in the calculation of the fin efficiency, the heat loss through the bottom of the collector is accounted for in by using the inverse of the R-value (i.e. k_{in}/L_{in}). A lower R-value corresponds to an increase in the overall heat loss coefficient as is the case for the BIT collector.

In relation to the side or edge where for the BIT design insulation does not exist, the heat loss, U_e, is referenced to the collector area. In an assumption case where both the BIT collector and BIPVT collector use insulation of identical thickness on the edges and bottom, the edge losses can be estimated by assuming one-dimensional sideways heat flow around the perimeter of the collector system (Duffie and Beckman, 2006). In this instance Equation 22 applies.

$$U_e = (UA)_{edge} / A \tag{22}$$

Where $(UA)_{edge}$ is the edge loss coefficient -area product and A is the collector area.

From this equation the differences between the areas of the tested collectors (i.e. 6 m^2 for BIT and 1 m^2 for BIPVT) indicates that there is substantially higher heat loss through the edges in the BIT compared with the BIPVT. Therefore, it can be said that a consideration for reducing the overall heat loss from the system would be to use edge (or side) insulation if possible and to consider perhaps a smaller collector area.

It was also identified that air spaces were present in the BIT design, shown in Figure 37. The BIT absorber was sitting on the polystyrene insulation and the spaces between the fluid channels and insulation were not insulated. This in effect, decreases the thermal resistance of the system, causing additional losses through forced convection as the heated fluid travels through the collector and natural convection from the fluid channels to the air space. The end caps sealing the top and bottom of the collector eliminate heat loss through forced convection because the air spaces become stagnant.

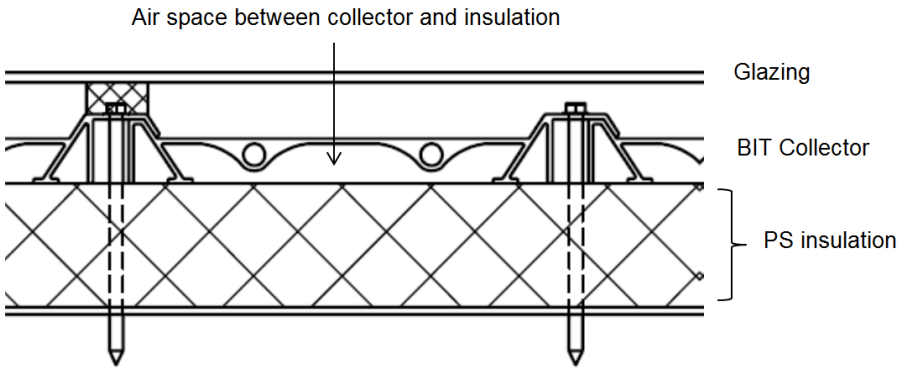

Figure 37: Front view showing the presence of air gaps.

An important specification for the BIT collector was that it had to replicate a typical metal long run roof. This is the reason for the BIT collector being designed in a specific way, so as to allow it to be integrated directly into a long run metal roof; as shown in Figure 38. In the case where the collector design is altered to have side insulation, complications could occur in terms of its 'intergratability'.

Figure 38: Typical long-run roofing construction (adapted from, Wahab, et al., 2011).

A possible solution however for overcoming the heat loss due to the presence of the air gap between the absorber and the rear insulation would be to use extruded polystyrene matching the profile of the collector, this would effectively eliminate this problem. Alternatively, loose filling insulation such as mineral wool, macerated paper or wool could be used which would also eliminate heat loss to the air space.

As such two possible avenues were available for the progression of the study. Firstly, the collector could be optimised by improving the rear and side insulation or secondly, using the current design to investigate how well it performs as a collector for water heating in a domestic system. The latter option was chosen because the simplicity of the design meets the basic configuration of a long run metal roof, meaning it can be integrated 'into rather than onto' (as recommended by Anderson, 2009) the roof, thus achieving a high level of integration (maintaining the building aesthetics). The reason for the first option being overlooked for this study, is that although the collector performance maybe

improved, it borders on the possibility of producing a standalone collector that would essentially be integrated ‘onto’ the roofing structure, thus contradicting the aims of this research.

3.3 Experimental Performance of BIT-SWH System

As stated previously, it was decided that instead of optimising the collector design the initial configuration would be used in a SWH system.

3.3.1 No load Performance

A good initial test to determine how well the BIT collector performs is to connect it to a SWH system and to observe the temperatures achieved in the storage tank when no load is drawn. This will give an indication of the temperatures reached within the tank, which is directly related to the effectiveness of the BIT collector for SWH. It was observed that for no load operation, temperatures as high as 68 °C could be achieved by the BIT-SWH system, as shown in Figure 39.

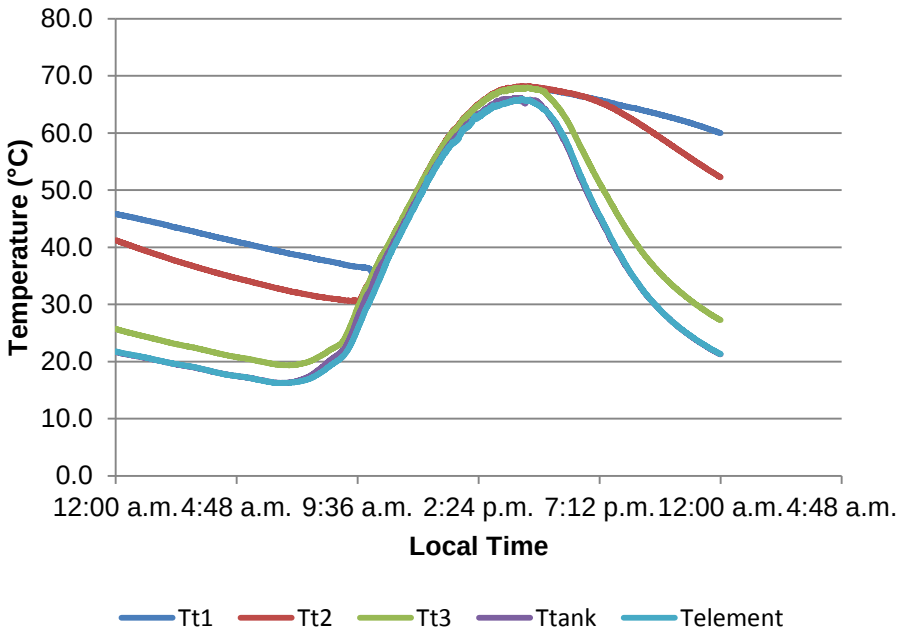

Figure 39: Storage tank temperature distribution.

Additionally, if we compare this to the temperatures reached by the collector, as shown in Figure 40, we can see that essentially all the heat gained by the collector is transferred directly into the storage tank. Therefore, it can be said that the configuration of the BIT-SWH system is effective when considering heat transferred from the collector to the storage tank. However, when considering previous studies such as that by (Wahab, et al., 2011) and work by Anderson (2009), this collector would be considered 'poorly' performing, in terms of the required temperatures for a domestic heating system. Additionally, the building code for New Zealand requires that the temperature of the water in the storage tank must reach at least 60 °C once each day (EECA, 2009).

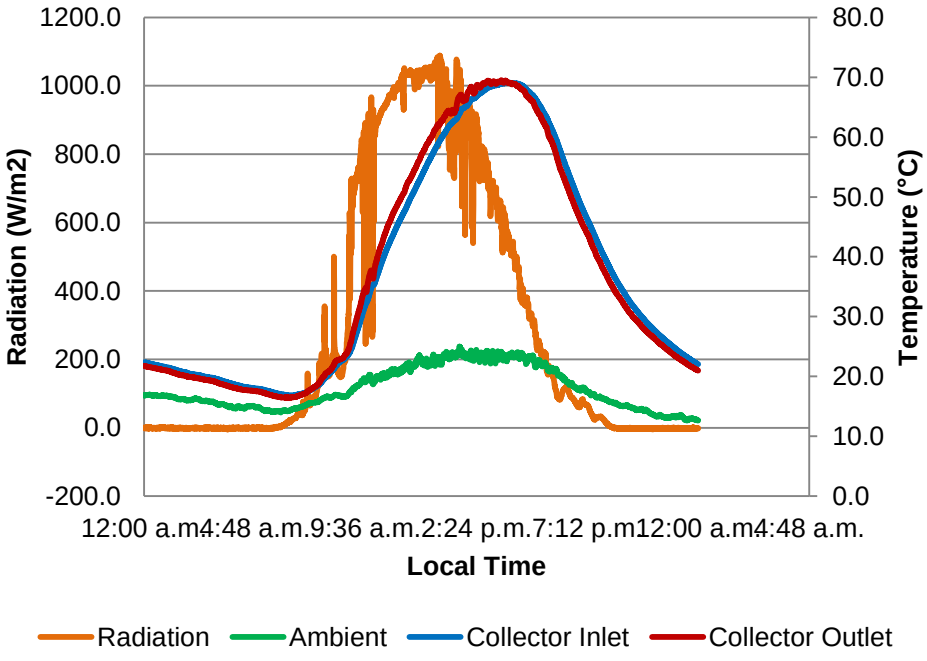

Figure 40: Collector temperatures and environment measurements.

The thermal efficiency for this collector has shown an improvement compared with the previous two studies. An optical efficiency of 75% compared with 45% for Wahab, et al. (2011) and 60 % for Anderson (2009), however the heat losses observed has greatly affected its performance. In comparison, a maximum tank temperature of under 70 °C is low, considering temperatures of around 90 °C could be obtained by the collector investigated by Wahab, et al. (2011). Additionally, higher heat loss (a slope of 23) is observed with this collector design, compared with previous designs (slopes of 4.1 and 5.6 for Wahab, et al., (2011) and Anderson (2009), respectively). Therefore it would be meaningless to conduct an experiment using a standardised load profile without addressing the issues affecting the heat loss in the collector.

3.3.2 Standard Load Profile Performance

It has been stated that an experiment using the BIT-SWH to investigate the performance of the collector would be meaningless, however from the viewpoint of the control system; such a test may provide interesting results. Therefore it was decided that an investigation into the effectiveness of the controller for use in a BIT-SWH would be undertaken.

It should be noted that the particular day this test was performed is not considered 'optimum' solar conditions, with an average solar insolation of 126 W/m^2 for the period where the test was performed between 8 am to 8 pm. The results for the tank temperature distribution are shown in Figure 41. Additionally, the collector temperatures and environmental conditions are shown in Figure 42.

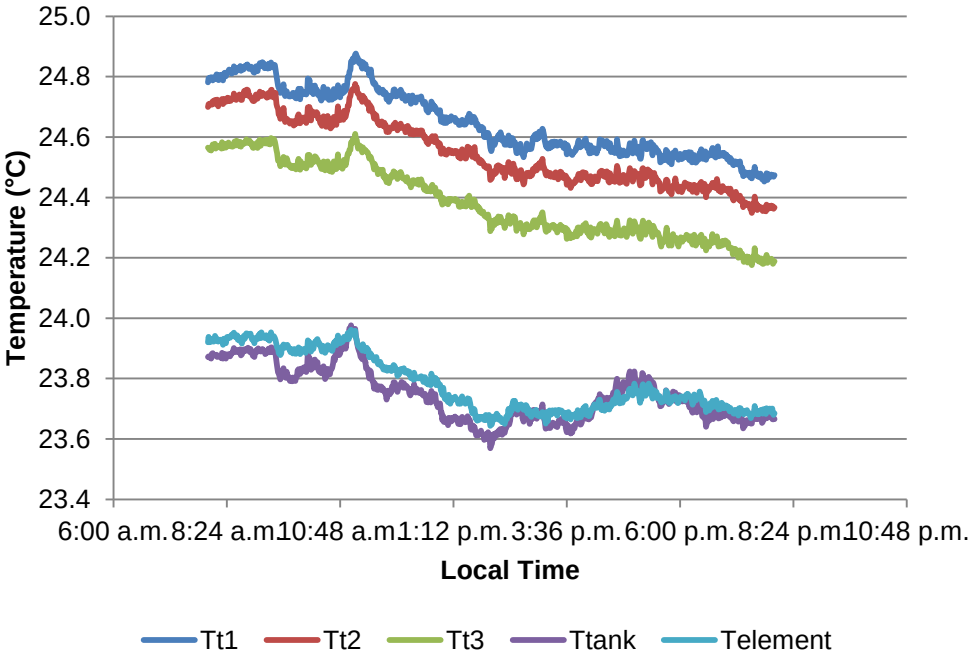

Figure 41: Storage tank temperature distribution for standardised load.

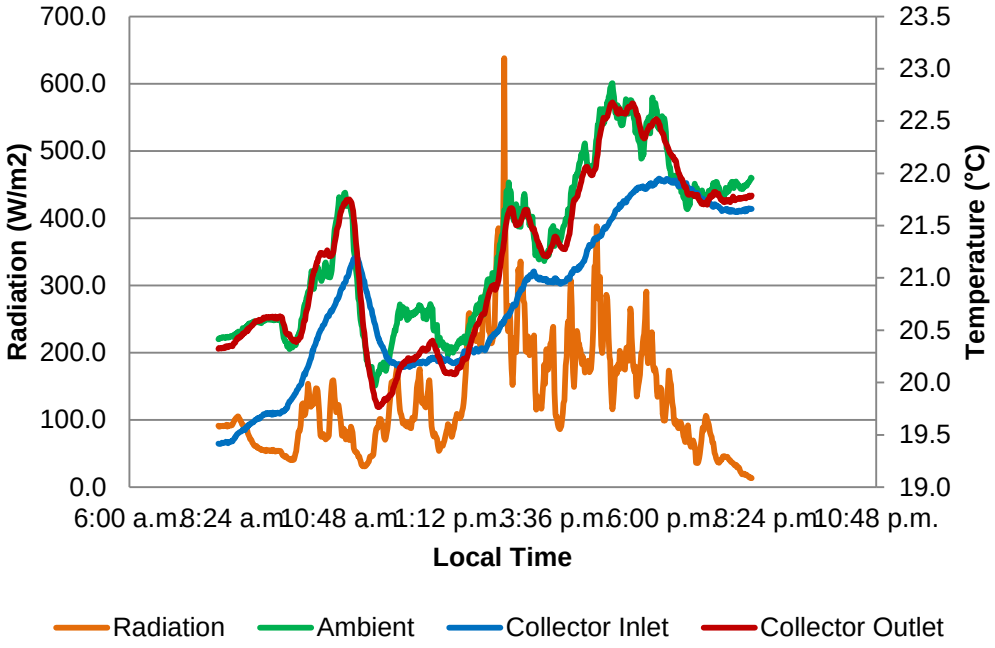

Figure 42: Collector temperature and environmental readings.

The controlling of the system pump and solenoid were based on the differential principle and standard load profile, respectively. It was observed that for the conditions of the testing period the parameters for meeting the algorithm for the pump were not fulfilled. The temperature difference needed to activate the pump was set at 8 °C; however as can be seen from Figure 41 and Figure 42, the values which dictate this difference (being collector outlet and tank cold region temperature, T_{tank}) doesn't actually produce a temperature difference. This is because the collector did not receive sufficient heat gains due to relatively low solar insolation. Similarly, the solenoid was never activated; this is largely due to the fact that there wasn't sufficient heat gain in the storage tank to supply to the load. Initially, the algorithm was configured to 'dump' different volumes of water so as to represent the load used by the household however; this was impractical due to the fact that the load needed is based on hourly requirements in terms of thermal energy (MJ/hr). Therefore the controller was reconfigured to dump a certain amount of energy at times specified by the standard profile. Because of the direct relation between the collector heat again and thermal energy applied to the tank, the signal to the solenoid valve remained closed. Details of the algorithm are provided in Appendix D.

Since the performance of the controller could not be determined using the experimental rig, a simplified theoretical version for the pump and solenoid, shown in Figure 43 and Figure 44 respectively, was developed allowing different cases to be applied. This would allow the effectiveness of the controller for use in a system such as the BIT-SWH to be investigated.

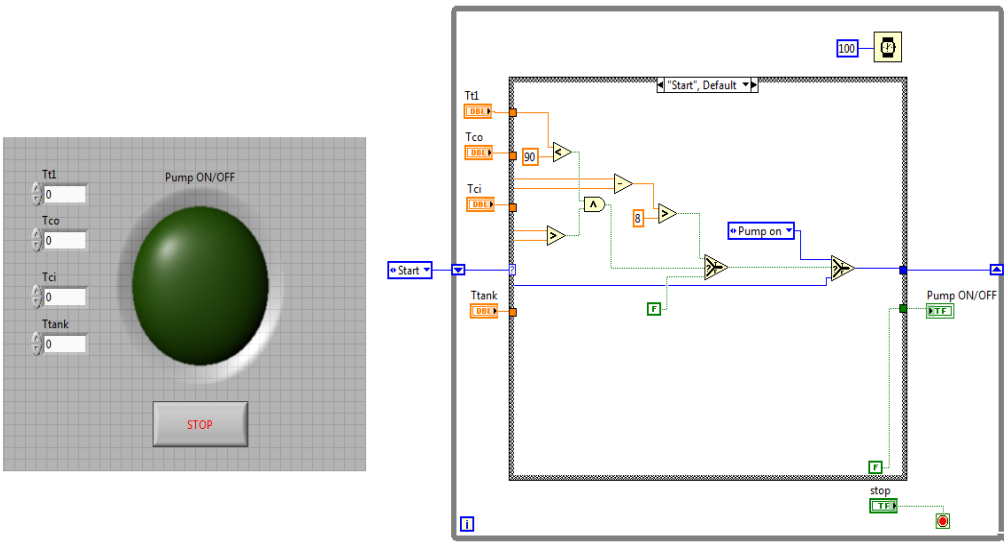

Figure 43: Simplified pump controller (left: front panel, right: block diagram).

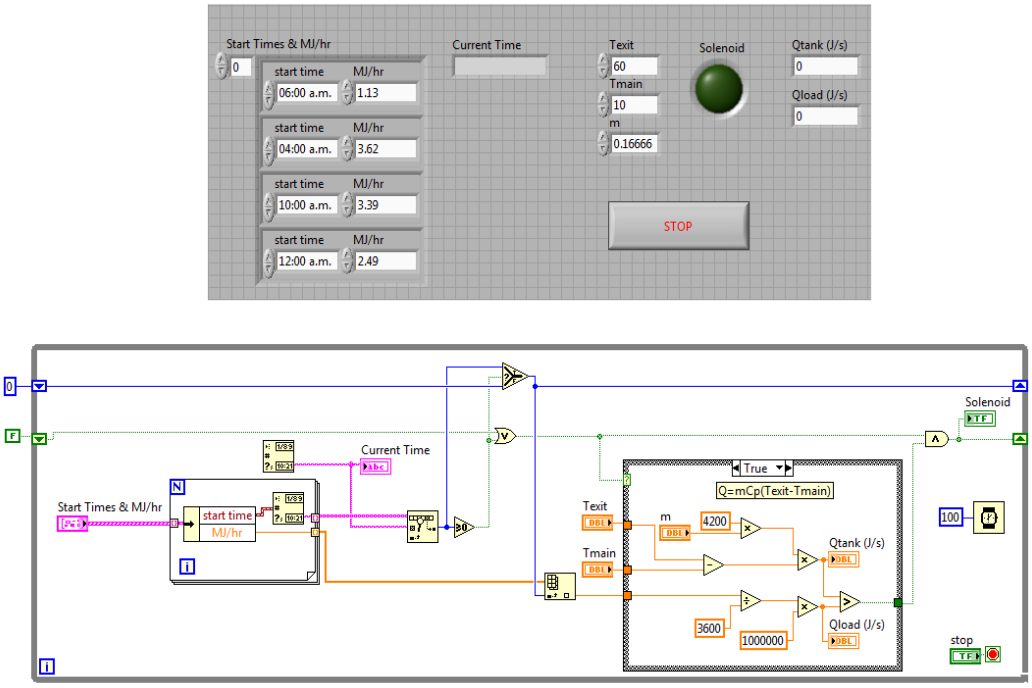

Figure 44: Simplified solenoid controller (top: front panel, bottom: block diagram).

For the pump the following cases of activation/deactivation were investigated: Temperature difference (ΔT) over 8 °C, below 4 °C and worst case scenario where the temperature in the hottest region of the tank (T_{t1}) exceeds 90 °C. The results from the theoretical controller showed promising results, with the pump (LED light) activating when the ΔT was greater than 8 °C and deactivated when the ΔT was less than 4 °C. The pump would also remain deactivated until the ΔT of 8 °C was reached again. This means that the pump would only activate if there was heat to be gained from the collector. Additionally, the pump remained deactivated for the worst case scenario when the temperature in the hottest region, T_{t1}, exceeded 90 °C even if there was heat to be gained from the collector. In contrast, the load controller activation is based on the current local time rather than parameters from the system. All the cases set out in the load profile, as shown in Table 1 were investigated.

Table 1: Load profile cases

Time	Hourly thermal load (MJ/hr)
6:00 a.m.	1.13
8:00 a.m.	3.62
10:00 a.m.	3.39
12:00 a.m.	2.49
2:00 p.m.	1.81
4:00 p.m.	1.58
6:00 p.m.	2.49
8:00 p.m.	2.94
10:00 p.m.	2.49
11:00 p.m.	0.68

Once the parameter for activation was met (the local time) load was drawn from the system, for example at 6:00 am a required load of 1.13 MJ/hr needs to be drawn. This was achieved by actively comparing the load value of 1.13 MJ/hr to the rate of heat extracted, Q_{tank}, from the tank, calculated using Equation 23. When the load matched the extracted energy, the valve would then shut. This would then be repeated for all time periods, thus replicating the standardised load profile.

$$Q_{tank} = m\, C_p\, (T_{exit} - T_{main}) \tag{23}$$

Where, m is the flow rate through the tank in kg/s and T_{exit} and T_{main} are the outlet and inlet temperatures, respectively, in °C.

For the tests, an approximate flow rate of 0.17 kg/s (10 L/min) was used; this was obtained by manually measuring the volume of mass exiting the tank within 60 seconds. Additionally, the inlet temperature was taken to be 10 °C and outlet as 60 °C which was manually decreased over time to simulate the cooling of the water in the tank as load was drawn.

The results from the theoretical controller indicated that this method of simulating the load for a household maybe impractical. For instance, if the highest and lowest load cases are considered, (8:00 am with an hourly load of 3.62 MJ/hr load and 11:00 pm with an hourly load of 0.68 MJ/hr, respectively) the required load based

on heat extracted from the tank can be calculated. Of the parameters in Equation 5, the temperature difference is the only parameter which varies (assuming constant flow rate). The results for the two extreme cases are summarised below (for all time periods refer to Appendix E).

8 am using 3.62 MJ/hr, ΔT = 1.4 °C required

11 pm using 0.68 MJ/hr, ΔT = 0.3 °C required

It can be seen that for the highest heat load, a temperature difference of 1.4 °C is needed before the amount of extracted heat from the matches that of the load. Moreover, for the lowest heat load, a temperature difference as low as 0.3 °C is required. This highlights a slight impracticality in the method. It is important to note however, that a big assumption made here is that the heat gain from the collector doesn't affect the temperatures within the tank. This would be untrue in an actual application. Unfortunately, this could not be investigated further with this system, due to time constraints and the collector being classified as 'poorly' performing. However, this exercise has shown that the controller is accurate and can be effective. What is also advantageous about the controller is that if perhaps a different approach was used compared to the method used here, a slight modification of the controller can be made to accommodate for this. With this mind, different aspects such as incorporating live weather data and automatic prediction of user water draw off (Prud'homme and Gillet, 2001) by implementing advanced control strategies. This would ultimately result in a well-managed, efficient system.

3.4 Experimental Summary

From the experimental testing of a BIT collector it was shown that an optical efficiency of 75% could be achieved, the downside to this is that high heat losses also occurred. It was identified that the major contributing factor to the heat loss was the lack of side insulation as well as air spaces present between the collector and the polystyrene insulation. Moreover, a possible solution was suggested for overcoming this by using extruded polystyrene sheets with a matching profile, thus eliminating the spaces of air and also extending to provide thermal resistance on the side. From a theoretical viewpoint of the glazed collector it was shown that the major contributions to the heat gain and heat loss of the system was the fin efficiency and overall heat loss coefficient, particularly the contribution of the bottom and side heat loss coefficients. Moreover, it was shown that the use of a higher thermal conductivity material does in fact increase the fin efficiency and subsequently the heat gain and thermal efficiency of the collector.

Additionally, it was decided that rather than optimise the BIT collector, experiments would be conducted to investigate its suitability in a domestic water heating application. The reason for this was largely due to the fact that the BIT collector was designed to replicate the roofing structure of a standard metal long run roof, which is typical of New Zealand house structures.

Results from the systems test when no load was drawn showed that temperatures of over 60 °C could be reached within the tank. A comparison with previous collectors used in water heating systems, particularly that of (Wahab, et al., 2011)

highlighted the potential pitfall of using a simple design, which would also suggest that the high heat loss from such a design has consequently adverse effects on it effectiveness for water heating. As such, it was decided that it would be impractical to investigate its use in a system replicating daily operation.

Another aspect of the BIT-SWH that was of interest was the control system. This is used for controlling both the pump and solenoid valve using temperature differential control and a standardised load profile. Although it was decided that it was impractical to run a replicate SWH system to characterise collector performance, from the viewpoint of the control system such as test was of interest. Unfortunately, the experimental tests in less than 'ideal' solar conditions failed to activate either of the controllers; therefore a theoretical approach was used to investigate its effectiveness.

From the theoretical tests conducted on the controllers, it was seen that the algorithm is indeed effective for controlling a BIT-SWH system. This is especially true for the temperature differential pump controller. Tests also showed that the 'dumping' controller was accurate but perhaps a different method to the one used would be more practical. Additionally, it was identified that there was potential to modify the collector to a more advanced strategy.

Chapter 4: Simulation of BIT-SWH System Performance

4.1 Introduction

A good way to assess the performance of the BIT-SWH system is to simulate its performance, allowing for a comparison between experimental and theoretical results. In order to assess the theoretical performance of the system, a simulation was performed using TRNSYS (Solar Energy Laboratory (SEL), 2008).

TRNSYS is a widely used software tool for conducting transient simulations of solar thermal energy systems using quasi-steady models. The mathematical representations of the components of the solar energy system are presented as algebraic or ordinary differential equation models, which the software interconnects depending on energy and mass flows. Its flexible nature allows the user to configure any number of systems and to determine their performance at a large number of sites worldwide. The advantage in the simulation conducted is that the actual global incident solar radiation which the system was exposed to can be used directly from recorded data allowing for an accurate comparison.

To demonstrate the performance of the BIT-SWH system it was modelled using the TRNSYS in-built example of a solar domestic hot water system based on a solar thermal collector (SDHW.tpf file), as shown in Figure 45. For the simulations the parameters for the BIT collector obtained from the efficiency calculations in the above chapter was used as inputs into the Type 1 collector. This was coupled to a stratified tank (Type 4) using input parameters also obtained from experimental results. The weather data for the global incident solar

radiation falling on the system was also used as the input for the Type 109 component, generally used for TMY data.

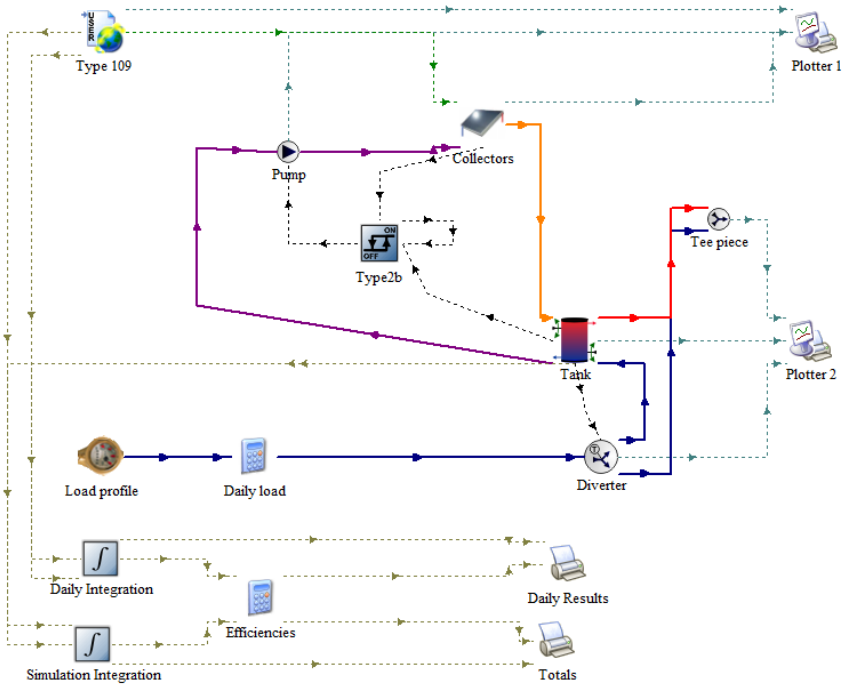

Figure 45: TRNSYS model of BIT-SWH system.

For the simulation the BIT-SWH was assumed suitable for use in a medium residence (4-5 occupants) in Hamilton, NZ. As such, the components used in the experimental BIT-SWH such as the collector with an area of 6m^2 mounted at 5° used in conjunction with a 180 L storage tank was assumed suitable. In terms of thermal load two cases were assessed, the first being when no load was drawn from the system, this test was only used as a way of validating the accuracy of the simulation otherwise this test is impractical. The second test used a standardised load profile. This allowed for the use of the hourly load profile of the system which was simulated in the experiments by controlling the solenoid valve. The profile used is based on a peak daily thermal load of 25.6 MJ/day which is typical of the load used in a medium sized New Zealand residence.

4.2 No Load Simulation

To assess the accuracy of the simulation a pre-requisite test was conducted for the no load situation. This would allow a comparison to be made with the no load results obtained from the experiments. The collector parameters used in the simulation as well as the environmental data obtained from the experiments were applied so as to provide comparable results.

From an observation of Figure 46 and Figure 47, it is evident that the simulation of the temperature distribution in the tank matches closely to that of the results obtained from experiments. The temperatures within the tank for the simulation reach temperatures of over 60 °C, which is similar to the experimental results. This result is also confirmed by the collector temperature readings and radiation plot, shown in Figure 48 for the simulation and Figure 49 for experimental. However, there is a slight difference in the results for the collector plots. This is due to the simulation only using the radiation readings for the period starting at 8 am through to 4 pm where the radiation readings are above 0 W/m^2. Aside from this, the temperatures predicted by the simulation of the collector reaching temperatures just below 70 °C have been confirmed experimentally. Therefore, it can be stated that this simulation model provides an accurate validation method for the performance of the BIT-SWH system.

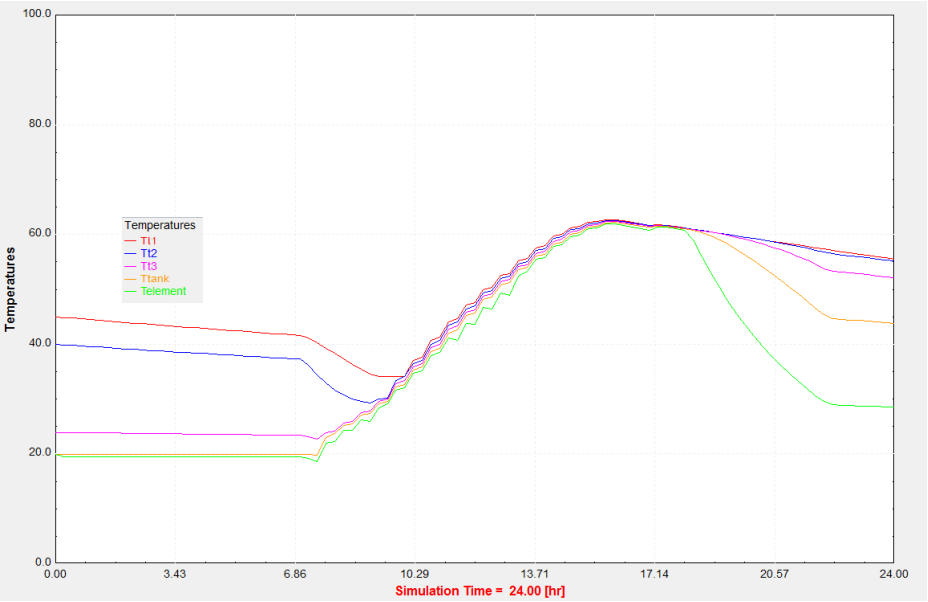

Figure 46: Simulation results of tank temperature distribution for no load.

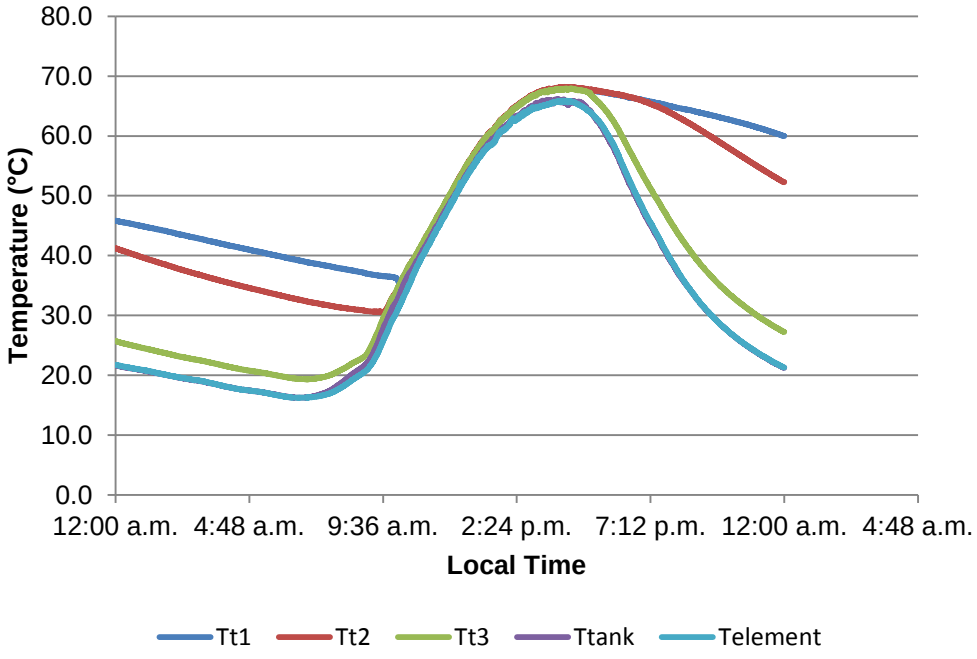

Figure 47: Experimental results of tank distribution for no load.

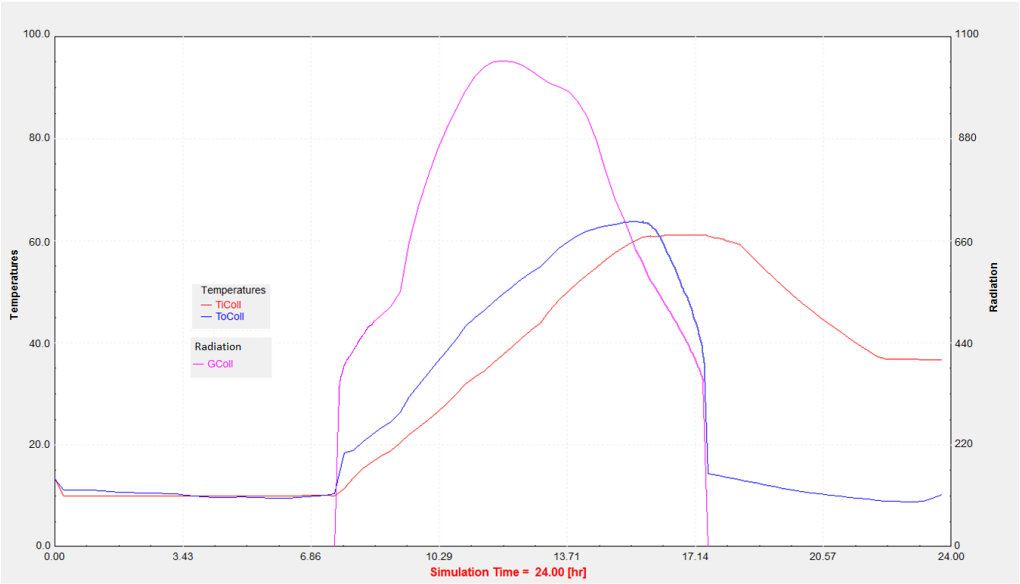

Figure 48: Simulated collector inlet and outlet temperature and radiation.

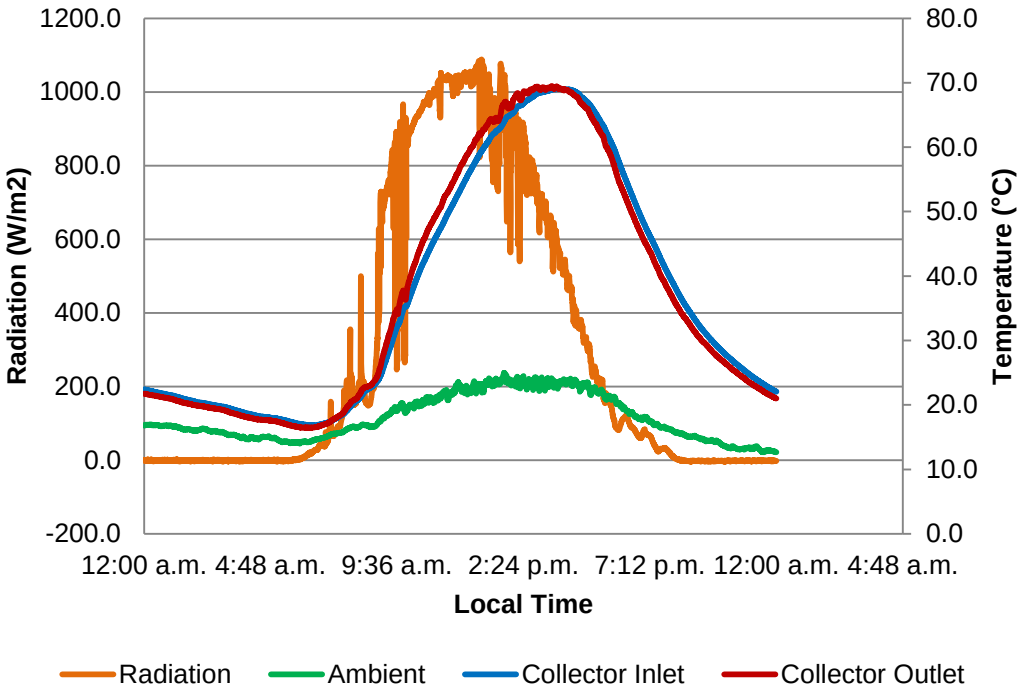

Figure 49: Measured collector temperatures and environment conditions.

4.3 Load Profile Simulation

Now that the simulation of a no load situation is complete, thus validating the method, a simulation can be carried out to predict the systems performance based on the standardised load profile. However, rather than use the efficiency equation of the 'poorly' performing BIT a hypothetical scenario was investigated.

In the case where the collector heat loss had been reduced, a hypothetical value of 5.55 for the heat loss was chosen such that it is comparable to a good performing integrated collector. These are shown by Equation 24 and Equation 25, representing the BIPVT collector investigated by Anderson (2009) and the modified BIT, respectively. This provides comparable results when running the simulation of the system operating under the standardised load. The weather data that was used was TMY data for Hamilton, New Zealand (Anderson, 2009).

$$\eta = 0.60 - 5.55\ (T_{ci} - T_a / G) \tag{24}$$

$$\eta = 0.75 - 5.55\ (T_{ci} - T_a / G) \tag{25}$$

The measurement of the performance of both collectors in water heating applications was characterised using solar fraction, (f), shown in Equation 26 (Duffie and Beckman, 2006). The solar fraction is the amount of energy provided by the solar water heating system divided by the total energy required.

$$f = L_S / L \tag{26}$$

Where, L_S is the load supplied by the SWH system and L is the required load.

Based on the collector efficiencies shown in Equations 24 and 25 it can be seen in Figure 50, that during a week of operation over a summer week, in this case in the month of January, there is a noticeable difference in the solar fractions. The BIT collector which has the sole purpose of heating water almost meets the load requirement achieving solar fractions as high as 98 % for the last three days of the week. This suggests that if the heat loss issues of the BIT are addressed, its performance will increase considerably.

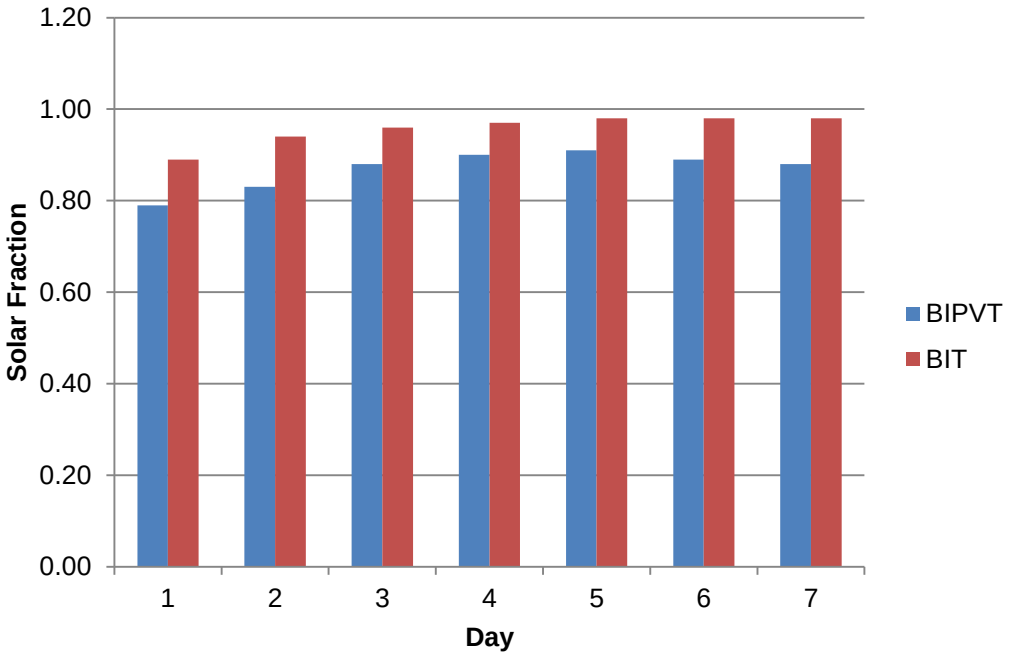

Figure 50: Solar fraction of BIPVT and BIT systems over summer.

If the simulation is also applied for a winter week, in this case TMY data for the month of June, it can be seen from Figure 51, that there is also a noticeable difference between the performances of the collectors compared with the summer week. The lower solar fraction values are due to the relatively low ambient conditions coupled with lower levels of solar radiation during winter (Anderson, 2009). That being said there is also a significant difference in the solar fractions

between the BIPVT-SWH system and BIT-SWH system. At its best the BIT-SWH system provided over 70 % of the required load which is shown for the final day of the week.

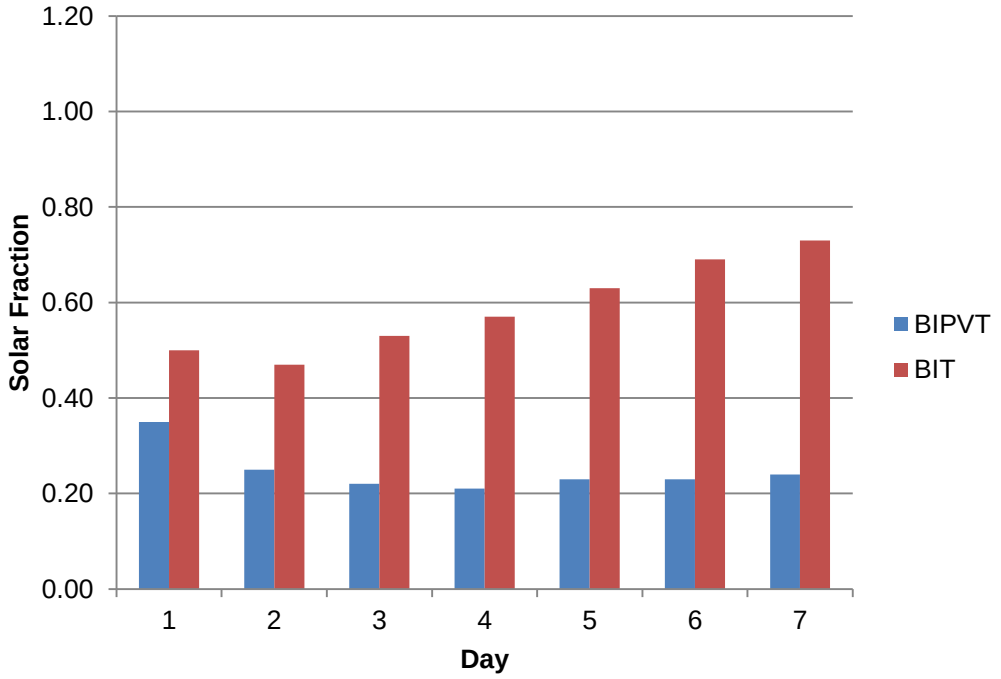

Figure 51: Solar fraction of BIPVT and BIT systems over winter.

In conclusion, there is strong evidence to suggest that if the heat loss of the BIT collector is reduced considerably (in this case from 13 down to 5) there will be a significant increase in its thermal performance. It is recommended that the issues relating to the high heat losses are addressed and resolved.

4.4 Simulation Summary

From the simulation modelling of the BIT-SWH system it is apparent that there are a number of issues to be addressed, particularly concerning the design of the collector.

It has been shown that the performance of the collector in an actual domestic water heating application, can be modelled accurately using the TRNSYS model. Furthermore, simulation results when no load was drawn from the systems show a good correlation between the predicted and actual performance.

The modelling of the collector in a hypothetical situation when load was drawn showed that by reducing the collector heat loss, possibly by using extruded insulation, significant improvement in its performance characterised by solar fraction can be achieved. The outcome of this finding is that the BIT-SWH system becomes a viable means of achieving a large portion of the daily hot water requirements of a domestic household.

Chapter 5: Conclusions and Recommendations of Future Work

5.1 Conclusions

The driving force of our world is energy and currently the majority of this demand is met by fossil fuels. Improvements in quality of life and rapid industrialisation in many countries are increasing energy demand significantly and the potential future gap between energy supply and demand is predicted to be large (Tian and Zhao, 2013). As a result, serious consideration needs to be made about the alternatives for current resources and its sustainability for the future.

It has been stated that the use of renewable energy, specifically solar energy, has the potential to generate all of the world's energy requirements many times over (Kreith and Goswami, 2007). This has led to an increased interest into the different methods with which radiant energy from the sun can be harnessed. An area that is predominant worldwide is the use of solar derived heat for water heating, which is largely dominated by the domestic sector. This is shown to be true, particularly in a country like New Zealand.

In this study an effort has been made to develop a new BIT collector and thus a BIT-SWH system, with the aims of providing an aesthetically uniform design and improved performance. It was shown that there are a number of key points to be observed particularly when constructing the collector where significant improvements can be made to the collector's performance. An issue that was observed with the collector design was the high heat losses caused by air spaces

and the lack of side insulation. Possible solutions for overcoming this may be to use extruded polystyrene insulation to match the collector profile. This would 'slot' into the underside eliminating air spaces. Any other improvements that reduce the heat loss from the collector, would contribute to increasing its thermal performance.

It was also decided that rather than optimise the collector, due to its simple construction, its viability for use in a domestic hot water heating system would be investigated. A comparison however, with a similar system concluded that the temperatures achieved by the system were relatively low. Moreover, a simulation model of the system using TRNSYS found that there was a good correlation between the predicted and actual, thus verifying a viable method for accurately predicting the system performance.

Since the current BIT collector design was considered as 'poorly' performing, a hypothetical case was also investigated using the TRNSYS model. In this case the heat losses in the collector were assumed to be comparable to that of a well performing integrated collector. The subsequent results of the simulation highlighted the importance of addressing the heat losses which significantly affect the collector's performance, particularly for water heating. Additionally, simulated results for the improved BIT system showed that for a summer week the collector could meet a high percentage of the hot water requirements for a medium sized residence in Hamilton. Furthermore, it was observed that for a

winter week the BIT-SWH system performed well when compared to a BIPVT-SWH system.

Furthermore, a theoretical test of the control strategy for the BIT-SWH system showed that the strategy used was a viable configuration for the control of a water heating system. This was especially true for the control of the pump in the collector loop. The tests also showed a slight impracticality in the method used for controlling the load, it was suggested that if an alternative method was used a slight modification of the controller could be made due it's the flexibility.

.

In summary this study has highlighted the potential for BIT collectors and BIT-SWH systems for meeting the heating requirements of New Zealand households, however careful consideration needs to be made into managing the heat losses of the collector and system. Additionally, the potential for controlling these systems was shown to be viable and provides the possibility for managing such systems to operate at increased efficiencies by using advanced control strategies.

5.2 Recommendations for Future Work

Aside from the remarks that have been made about improvements to the collector and system, there are a number of opportunities in the area of solar thermal, particularly building integrated and domestic water heating, for which further work can be applied.

New Zealand's closest neighbour, Australia, is a world leader in the solar thermal industry. Therefore, renewable derived energy systems are essentially a large part of the development within the country. It would be of interest to compare how such a widespread adoption of solar technologies has occurred and how this can be achieved in New Zealand. A study investigating the possible barriers faced by New Zealand can provide interesting insight.

It was observed that for this integrated collector, the high level of integration that was achieved, boarders into the building and construction industry. If perhaps the technology is to be adopted, from a technical point of view an investigation into how such systems would fit into the current building regulations or if modifications are required, may prove useful. That being said, this would also relate directly to the heat and mass transfers that occur within the 'built' environment. In this context, if the BIT is used on a standard metal long run roof, an aluminium heat absorbing material is in 'direct' contact with standard roofing coloured steel. The implications of having heat transfer by having metals with dissimilar thermal conductivity, in contact would be of interest.

Additionally, the thermal expansion of roofing structures is a phenomenon observed in the roofing industry, a study into how this would be accounted for with integrated collectors would provide useful insight.

Finally, it was noted that there is currently no set configuration for integrated water heating systems. An optimisation study of systems relating to integrated collectors will significantly aid in the widespread adoption of architecturally uniform collectors and systems. It is also recommended that the area of system control be seriously addressed as it provides further opportunity for acceptance of solar water heating systems. A possible approach to this statement would be to use advanced control strategies.

REFERENCES

Adelhelm, R., and Berger, D. (2003). *Requirements for a large area solar simulator regarding the measurement of MJ solar cells*.

Anderson, T. N. (2004). *Advanced Heat Pump Water Heaters.* ME, University of New South Wales, Sydney.

Anderson, T. N. (2009). *Investigation of Thermal Aspects of Building Integrated Photovoltaic/Thermal Solar Collectors.* PhD, The University of Waikato, Hamilton.

Anderson, T. N., Duke, M., Morrison, G. L., and Carson, J. K. (2009). Performance of a building integrated photovoltaic/thermal (BIPVT) solar collector. *Solar Energy*, *83*(4), 445-455.

Arvizu, D., Balaya, P., Cabeza, L. F., Hollands, K. G. T., Jäger-Waldau, A., Kondo, M., Konseibo, C., Meleshko, V., Stein, W., Tamaura, Y., Xu, H., and Zilles, R. (2011). Direct Solar Energy. In O. Edenhofer, R. Pichs-Madruga, Y. Sokona, K. Seyboth, P. Matschoss, S. Kadner, T. Zwickel, P. Eickemeier, G. Hansen, S. Schlömer & C. von Stechow (Eds.), *IPCC Special Report on Renewable Energy Sources and Climate Change Mitigation*. Cambridge, United Kingdom and New York, NY, USA: Cambridge University Press.

Assoa, Y. B., Menezo, C., Fraisse, G., Yezou, R., and Brau, J. (2007). Study of a new concept of photovoltaic–thermal hybrid collector. *Solar Energy*, *81*(9), 1132-1143.

Bauser, M., and Siegert, K. (2006). *Extrusion*: A S M International.

Bhardwaj, R. K., Gupta, B. K., and Prakash, R. (1967). Performance of a flat-plate solar collector. *Solar Energy, 11*(3–4), 160-162.

Bliss Jr, R. W. (1959). The derivations of several "Plate-efficiency factors" useful in the design of flat-plate solar heat collectors. *Solar Energy, 3*(4), 55-64.

Bondor. (2013). *Creating New Dimensions in Sustainable Building Technologies*. from http://www.bondor.co.nz/brochures/444437001242620644.pdf

Bynum, R. T. (2001). *The Insulation Handbook*: McGraw-Hill.

Close, D. J. (1962). The performance of solar water heaters with natural circulation. *Solar Energy, 6*(1), 33-40.

Cox, C. H., and Raghuraman, P. (1985). Design considerations for flat-plate-photovoltaic/thermal collectors. *Solar Energy, 35*(3), 227-241.

da Silva, R. M., and Fernandes, J. L. M. (2010). Hybrid photovoltaic/thermal (PV/T) solar systems simulation with Simulink/Matlab. *Solar Energy, 84*(12), 1985-1996.

Duffie, J. A., and Beckman, W. A. (2006). *Solar Engineering of Thermal Processes*: John Wiley & Sons.

Edenhofer, O., Pichs-Madruga, R., and Sokona, Y. (2011). *Renewable Energy Sources and Climate Change Mitigation: Special Report of the Intergovernmental Panel on Climate Change*: Cambridge University Press.

EECA. (2009). Energy Efficiency and Renewable Energy in New Zealand, Year Six Report: March 2001 to 2007. Wellington: Monitoring and Technical Group, Energy Efficiency and Conservation Authority.

Garg, H. P. (1987). *Advances in Solar Energy Technology: Volume 1: Collection and Storage Systems*: Springer.

Garg, H. P., Shukla, A. R., Madhuri, I., Agnihotri, R. C., and Chakravertty, S. (1985). Development of a simple low-cost solar simulator for indoor collector testing. *Applied Energy, 21*(1), 43-54.

Gari, H. N., and Loehrke, R. I. (1982). Controlled Buoyant Jet for Enhancing Stratification in a Liquid Storage Tank. *Journal of Fluids Engineering, Transactions of the ASME, 104*(4), 475-481.

Ghani, F., Duke, M., and Carson, J. K. (2012). Effect of flow distribution on the photovoltaic performance of a building integrated photovoltaic/thermal (BIPV/T) collector. *Solar Energy, 86*(5), 1518-1530.

Gillett, W. B. (1980). The equivalence of outdoor and mixed indoor/outdoor solar collector testing. *Solar Energy, 25*(6), 543-548.

Goswami, D. Y., Kreith, F., and Kreider, J. F. (2000). *Principles of Solar Engineering*: Taylor & Francis Group.

Green, M. A., and Keevers, M. J. (1995). Optical properties of intrinsic silicon at 300 K. *Progress in photovoltaics, 3*(3), 189-192.

Gupta, C. L., and Garg, H. P. (1968). System design in solar water heaters with natural circulation. *Solar Energy, 12*(2), 163-182.

Harley, B. (2002). *Insulate & Weatherize: Expert Advice from Start to Finish*: Taunton Press.

Harrison, J., Tiedmann, T., and Center, F. S. E. (1985). *Solar Water Heating Options in Florida*: Florida Solar Energy Center.

Hottel, H., and Woertz, B. (1942). Performance of flat-plate solar-heat collectors. *Trans ASME (Am Soc Mech Eng), 64*, 91-104.

Hsieh, C. K., and Coldewey, R. W. (1974). Study of thermal radiative properties of antireflection glass for flat-plate solar collector covers. *Solar Energy, 16*(2), 63-72.

Jordan, U., and Furbo, S. (2005). Thermal stratification in small solar domestic storage tanks caused by draw-offs. *Solar Energy, 78*(2), 291-300.

Kalogirou, S. A. (2004). Solar thermal collectors and applications. *Progress in Energy and Combustion Science, 30*(3), 231-295.

Kalogirou, S. A. (2009). *Solar Energy Engineering: Processes and Systems*: Elsevier Science.

Kreith, F., and Goswami, D. Y. (2007). *Handbook of Energy Efficiency and Renewable Energy*: Taylor & Francis.

Kreith, F., and Kreider, J. F. (1978). *Principles of solar engineering*: Hemisphere Pub. Corp.

Kumar, R., and Rosen, M. A. (2011). A critical review of photovoltaic–thermal solar collectors for air heating. *Applied Energy, 88*(11), 3603-3614.

Lavan, Z., and Thompson, J. (1977). Experimental study of thermally stratified hot water storage tanks. *Solar Energy, 19*(5), 519-524.

Lloyd, C. R. (2001). Renewable energy options for hot water systems in remote areas. *Renewable Energy, 22*(1–3), 335-343.

Lloyd, C. R., and Kerr, A. S. D. (2008). Performance of commercially available solar and heat pump water heaters. *Energy Policy, 36*(10), 3807-3813.

Lovegrove, K., and Stein, W. (2012). *Concentrating Solar Power Technology: Principles, Developments and Applications*: Woodhead Pub Limited.

Mathur, K. N., Khanna, M. L., Davey, T. N., and Sun, S. P. (1959). Domestic solar water heaters. *J Sci Ind Res, A18*, 51-58.

Meduna, V. (2013). Wind and Solar Power - Solar Energy.

Medved, S., Arkar, C., and Černe, B. (2003). A large-panel unglazed roof-integrated liquid solar collector—energy and economic evaluation. *Solar Energy, 75*(6), 455-467.

Morrison, G., Devakul, D., Tran, H., and Litvak, A. (1984). Solar Hot Water System Performance in the Bonnyrig Solar Village. *Report 1984/FMT/3*.

Morrison, G. L. (2012). TRNAUS 12.1 TRNSYS Extensions For Solar Water Heating. *Report by School of Mechanical Engineering*.

Munari Probst, M., and Roecker, C. (2007). Towards an improved architectural quality of building integrated solar thermal systems (BIST). *Solar Energy, 81*(9), 1104-1116.

Nahar, N. M., and Garg, H. P. (1980). Free convection and shading due to gap spacing between an absorber plate and the cover glazing in solar energy flat-plate collectors. *Applied Energy, 7*(1–3), 129-145.

Nahar, N. M., and Garg, H. P. (1981). Selective coatings on flat-plate solar collectors. *Renew Energy, 3*, 37-51.

Patil, P. G. (1975). Field performance and operation of a flat-glass solar heat collector. *Solar Energy, 17*(2), 111-117.

Pollard, A. R., Camilleri, M. T., French, L. J., and Isaacs, N. P. (2005). *How Are Solar Heaters Used in New Zealand?* Paper presented at the Proceedings of the Solar 2005 ANZSES Conference, Dunedin. www.branz.co.nz/cms_show_download.php?id=493c8b7eea0447f1c2b4ed24f2965b9aaa7f8303

Pollard, A. R., and Zhao, J. (2008). The Performance of Solar Water Heaters in New Zealand *Study Report 188*. Judgeford, Wellington: BRANZ Ltd.

Prud'homme, T., and Gillet, D. (2001). Advanced control strategy of a solar domestic hot water system with a segmented auxiliary heater. *Energy and Buildings, 33*(5), 463-475.

Raisul Islam, M., Sumathy, K., and Ullah Khan, S. (2013). Solar water heating systems and their market trends. *Renewable and Sustainable Energy Reviews, 17*(0), 1-25.

Richards, J. W. (2009). *Aluminium: Its History, Occurrence, Properties, Metallurgy and Applications, Including Its Alloys*: BiblioLife.

Shariah, A. M., and Ecevit, A. (1995). Effect of hot water load temperature on the performance of a thermosyphon solar water heater with auxiliary electric heater. *Energy Conversion and Management, 36*(5), 289-296.

Shariah, A. M., and Löf, G. O. G. (1997). Effects of auxiliary heater on annual performance of thermosyphon solar water heater simulated under variable operating conditions. *Solar Energy, 60*(2), 119-126.

Smyth, M., Eames, P. C., and Norton, B. (2006). Integrated collector storage solar water heaters. *Renewable and Sustainable Energy Reviews, 10*(6), 503-538.

Solar Energy Laboratory (SEL). (2008). TRNSYS 16.1 User Manuals.

Stoecklein, A. (2005). Cost Benefit Analysis for Solar Water Heating Systems *BRANZ Report EC1112*. Judgeford, Wellington: BRANZ.

Synergy Applied Research. (1985). The Promotion of Solar Water Heating Systems. (NZERDC Report 121).

Synergy Applied Research. (1986). In-situ Performance of Solar Water Heaters. (NZERDC Report 130).

Thomas, S., and Lloyd, C. (2005). *Experimental and Simulated Performance of Commercially Available Solar and Heat-pump Water Heaters in New Zealand.* Paper presented at the Proceeding of the Solar 2005 ANZSES Conference, Dunedin.

Tian, Y., and Zhao, C. Y. (2013). A review of solar collectors and thermal energy storage in solar thermal applications. *Applied Energy, 104*, 538-553.

Tiedemann, T. F., and Maytrott, C. W. (1997). *Indoor testing using a large area solar simulator*.

van Koppen, C. W. J., Thomas, J. P. S., and Veltkamp, W. B. (1979). Actual Benefits of Thermally Stratified Storage in a Small and a Medium Size Solar System. *Electric Power Research Institute (Report) EPRI EA*, 576-580.

Wahab, H. A., Duke, M., Carson, J. K., and Anderson, T. (2011). *Studies of control strategies for building integrated solar energy system*.

Weiss, W., and Mauthner, F. (2012). Markets and Contribution to the Energy Supply 2010. (Edition 2012).

Weston A, H. (2006). Quantifying global exergy resources. *Energy, 31*(12), 1685-1702.

Whillier, A. (1963). Plastic covers for solar collectors. *Solar Energy, 7*(3), 148-151.

Whillier, A., and Saluja, G. (1965). Effect of materials and construction details on the thermal performance of solar water heaters. *Solar Energy, 9*(1), 21-26.

Winegarner, R. M. (1976). Heat Mirror - A Practical Alternative to the Selective Absorber.

Appendix A: Tested BIT and BIT-SWH parameters

Table 2: Experimental BIT physical characteristics.

Parameter	Symbol	Value	Unit
Number of covers	N	1 or 0	
Number of channels per panel	n	2	
Channel diameter	D	5	mm
Channel Spacing	W	72	mm
Hose diameter	d_h	20	mm
Collector Length	L_c	2	m
Collector Width	w_c	1.13	m
Collector Area (Gross)	A_G	2.26	m^2
Absorber thickness	t	3.75	mm
Absorber Conductivity (Dals Steel Metal Pty Ltd, 2011)	k_A	209	W/mK
Insulation Thickness	L_{in}	50	mm
Insulation Conductivity (Bondor, 2013)	k_i	0.037	W/mK
Mounting Angle	β	37	°C

Table 3: Experimental BIT-SWH physical characteristics

Component and parameter	Symbol	Value	Unit
Collector			
Number of covers	N	1 or 0	
Number of channels per panel	n	2	
Channel diameter	D	5	mm
Channel Spacing	W	72	mm
Hose diameter	d_h	20	mm
Collector Length	L_c	6	m
Collector Width	w_c	1.13	m
Collector Area (Gross)	A_G	6.78	m^2
Absorber thickness	t	3.75	mm
Absorber Conductivity (Dals Steel Metal Pty Ltd, 2011)	k_a	209	W/mK
Insulation Thickness	L_{in}	50	mm
Insulation Conductivity (Bondor, 2013)	k_{in}	0.037	W/mK
Mounting Angle	β	5	degrees
Drain back tank			
Volume	V_{db}	45	L
Maximum working pressure	p_{max}	76	kPa
Storage tank			
Tank volume	V_{st}	172	L
Standing heat loss	t_{loss}	1.6	kWh/day
Pump			
Maximum power	P_{max}	90	W

Appendix B: Collector and System Testing Schematics

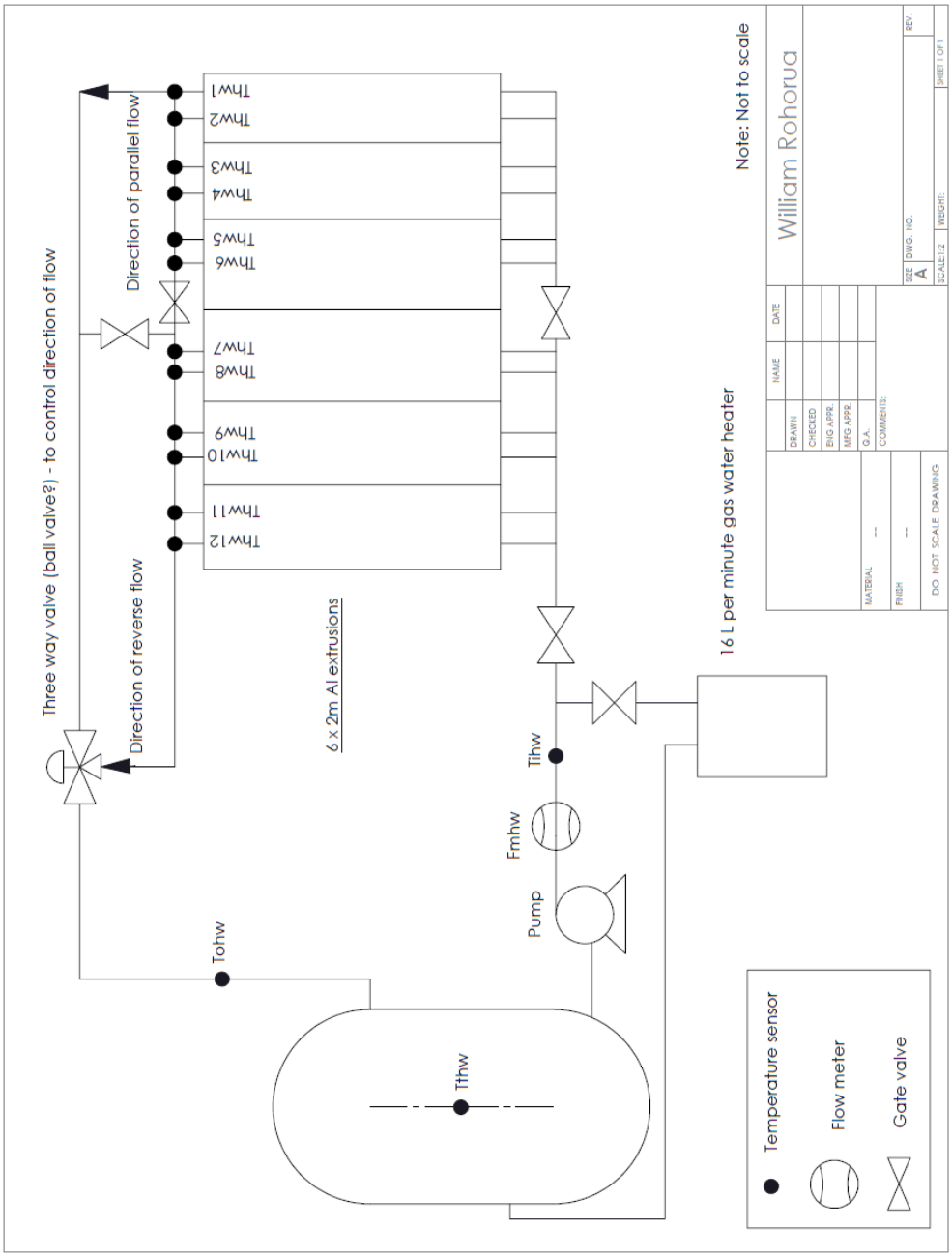

Figure 52: Schematic of BIT collector testing rig.

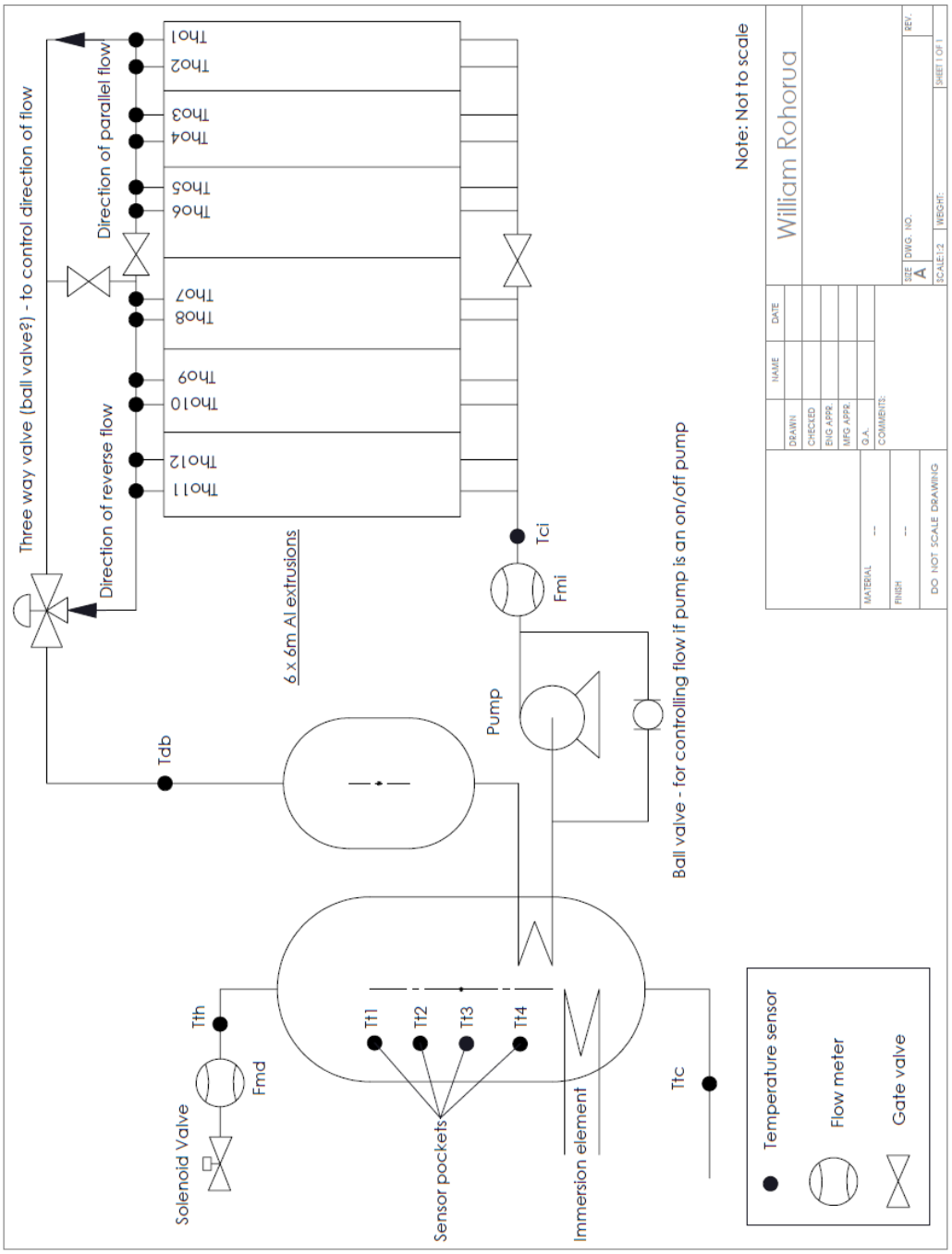

Figure 53: Schematic of BIT-SWH system testing rig.

Appendix C: Collector Testing Experimental Data

Table 4: Unglazed BIT collector data

Ambient Temp (°C)	Irradiance (W/m^2)	Inlet Temp (°C)	Outlet Temp (°C)	Mass flow rate (kg/s)	Instantaneous heat gain (Q)	Instantaneous efficiency
23.5	936.6	27.1	37.5	0.02	873.4	0.39
23.4	938.1	27.1	37.7	0.02	894.0	0.39
23.3	939.1	27.1	37.8	0.02	902.0	0.40
23.3	940.7	27.1	37.7	0.02	892.7	0.39
23.3	942.0	27.1	37.6	0.02	882.2	0.39
23.3	943.0	27.1	37.3	0.02	854.6	0.37
23.3	943.5	27.2	37.6	0.02	877.2	0.38
23.3	943.7	27.2	37.3	0.02	852.5	0.37
23.3	945.3	27.2	37.2	0.02	845.0	0.37
23.2	946.3	27.2	37.6	0.02	876.1	0.38
23.3	946.6	27.2	37.7	0.02	884.1	0.39
23.3	947.5	27.2	37.6	0.02	877.9	0.38
23.5	950.2	27.2	37.8	0.02	890.6	0.39
23.6	948.9	27.3	38.1	0.02	907.4	0.40
23.7	949.6	27.3	38.4	0.02	929.7	0.40
23.8	949.1	27.4	38.2	0.02	913.3	0.40
23.9	951.2	27.4	38.5	0.02	936.8	0.41
23.8	951.1	27.3	38.5	0.02	940.2	0.41
23.8	950.9	27.3	38.6	0.02	944.4	0.41
23.8	953.7	27.4	38.7	0.02	953.5	0.41
23.8	953.7	27.4	38.5	0.02	937.4	0.41
23.9	952.5	27.4	38.7	0.02	947.9	0.41
24.0	957.3	27.6	38.5	0.02	916.3	0.40
24.0	955.2	27.5	38.3	0.02	907.9	0.39
23.9	955.5	27.5	38.5	0.02	920.1	0.40
24.0	954.8	27.6	38.6	0.02	924.8	0.40
24.2	957.6	27.7	38.5	0.02	913.2	0.39
24.2	957.5	27.7	38.2	0.02	884.1	0.38
24.2	959.1	27.7	38.4	0.02	892.2	0.38
26.3	1016.7	49.2	50.6	0.02	121.0	0.05
26.3	1018.1	49.2	50.8	0.02	134.7	0.05
26.2	1021.3	49.2	50.7	0.02	130.7	0.05
26.3	1022.4	49.1	50.8	0.02	140.0	0.06
26.4	1022.9	49.1	50.8	0.02	142.2	0.06
26.4	1023.7	49.0	50.9	0.02	159.3	0.06
26.3	1022.6	48.9	51.0	0.02	169.2	0.07
26.3	1023.4	48.8	51.1	0.02	188.1	0.08
26.2	1025.0	48.7	51.0	0.02	188.5	0.08
26.2	1024.0	48.7	51.0	0.02	187.3	0.08

26.2	1022.4	48.7	50.9	0.02	181.8	0.07
26.2	1023.7	48.7	50.9	0.02	187.7	0.08
26.3	1022.9	48.7	51.0	0.02	198.2	0.08
26.3	1024.0	48.7	50.8	0.02	173.5	0.07
26.3	1022.4	48.8	50.8	0.02	168.0	0.07
26.1	1021.4	48.8	50.7	0.02	164.8	0.07
26.0	1021.9	48.9	50.6	0.02	144.7	0.06
26.0	1019.8	48.9	50.5	0.02	131.9	0.05
26.1	1019.4	49.1	50.6	0.02	124.6	0.05
26.0	1020.1	49.2	50.5	0.02	110.3	0.04
26.3	1018.1	49.3	50.5	0.02	107.3	0.04
26.6	1019.1	49.0	50.3	0.02	109.3	0.04
26.6	1020.1	49.1	50.5	0.02	114.7	0.05
26.5	1019.4	49.1	50.4	0.02	105.7	0.04
26.4	1021.4	49.2	50.5	0.02	114.1	0.05
26.5	1022.2	49.2	50.6	0.02	117.9	0.05
26.6	1021.1	49.3	50.8	0.02	123.7	0.05
26.6	990.3	57.3	57.9	0.02	44.0	0.02
26.7	993.2	57.2	58.0	0.02	63.8	0.03
26.7	988.8	57.0	58.1	0.02	89.1	0.04
26.8	986.8	56.9	58.2	0.02	104.2	0.04
26.8	985.8	56.9	58.2	0.02	109.2	0.05
26.8	983.5	56.9	58.1	0.02	100.3	0.04
26.9	982.9	57.1	58.0	0.02	80.0	0.03
26.8	982.5	57.3	58.1	0.02	69.2	0.03
26.6	982.9	57.5	58.2	0.02	59.9	0.03
26.5	983.4	57.8	58.2	0.02	39.3	0.02
26.2	983.9	57.0	58.2	0.02	96.3	0.04
26.3	979.1	57.3	58.2	0.02	79.8	0.03
26.5	979.1	57.5	58.1	0.02	52.1	0.02

Table 5: Glazed BIT collector data

Ambient Temp (°C)	Irradiance (W/m^2)	Inlet Temp (°C)	Outlet Temp (°C)	Mass flow rate (kg/s)	Instantaneous heat gain (Q)	Instantaneous efficiency
27.6	996.5	27.8	32.8	0.097	2001.5	0.83
27.6	998.8	27.8	32.6	0.097	1952.7	0.81
27.6	998.3	27.8	32.6	0.097	1925.4	0.80
27.6	998.0	27.8	32.5	0.097	1879.6	0.78
27.6	1002.1	27.8	32.4	0.097	1873.1	0.77
27.7	1001.4	27.8	32.4	0.097	1881.7	0.78
27.7	1001.6	27.8	32.4	0.097	1869.6	0.77
27.8	1003.4	27.8	32.4	0.097	1854.6	0.76
27.8	1001.6	27.9	32.4	0.097	1842.9	0.76
27.9	1000.1	27.9	32.4	0.097	1832.3	0.76
27.8	1002.6	27.8	32.4	0.097	1848.0	0.76
27.6	1002.2	27.9	32.4	0.097	1830.9	0.75
27.6	1001.1	27.9	32.4	0.097	1834.8	0.76
27.5	1001.7	27.9	32.4	0.097	1828.3	0.75
27.3	1002.7	27.9	32.4	0.097	1825.1	0.75
27.3	1003.4	28.0	32.5	0.097	1829.7	0.75
27.3	1000.1	28.0	32.5	0.097	1827.3	0.76
27.2	1009.4	28.0	32.5	0.097	1810.9	0.74
27.0	1009.0	28.1	32.5	0.097	1812.8	0.74
26.8	1008.8	28.1	32.5	0.097	1814.1	0.74
26.7	1012.6	28.1	32.6	0.097	1822.9	0.74
26.7	1016.2	28.0	32.5	0.097	1821.6	0.74
26.7	1013.9	28.1	32.5	0.097	1812.7	0.74
26.7	1014.4	28.1	32.5	0.097	1795.3	0.73
26.9	1017.8	28.2	32.6	0.097	1793.8	0.73
29.0	1000.9	44.6	46.8	0.097	903.3	0.37
29.3	1005.8	44.6	46.7	0.097	869.3	0.36
29.4	1005.0	44.5	46.6	0.097	843.3	0.35
29.5	1004.0	44.5	46.6	0.097	846.0	0.35
29.5	1004.0	44.5	46.5	0.097	819.7	0.34
29.5	1001.9	44.4	46.4	0.097	808.6	0.33
29.5	1003.4	44.4	46.3	0.097	774.2	0.32
29.5	1001.6	44.4	46.3	0.097	758.0	0.31
29.6	1003.2	44.5	46.3	0.097	740.3	0.30
29.7	1006.0	44.4	46.3	0.097	735.6	0.30
29.6	997.3	44.5	46.4	0.097	731.3	0.30
29.5	1002.4	44.6	46.5	0.097	745.5	0.31
29.6	1005.7	44.6	46.3	0.097	707.9	0.29
29.6	1002.7	44.5	46.1	0.097	651.4	0.27
29.4	1033.2	56.1	57.2	0.097	462.0	0.18
29.3	1029.3	56.1	57.2	0.097	452.9	0.18
29.2	1030.3	56.3	57.4	0.097	413.8	0.17

29.2	1033.2	56.3	57.3	0.097	391.1	0.16
28.9	1041.4	56.4	57.2	0.097	353.2	0.14
28.8	1035.5	56.4	57.2	0.097	327.0	0.13
28.8	1036.8	56.4	57.3	0.097	339.7	0.14
28.6	1033.7	56.6	57.3	0.097	313.2	0.13
28.7	1033.4	56.4	57.3	0.097	361.4	0.14
28.8	1033.1	56.4	57.2	0.097	326.8	0.13
28.9	1030.6	56.4	57.2	0.097	317.9	0.13
29.0	1036.2	56.3	57.2	0.097	337.7	0.13
29.1	1036.3	56.3	57.1	0.097	324.7	0.13
29.1	1037.5	56.1	57.0	0.097	359.6	0.14
29.0	1038.6	56.0	56.9	0.097	378.5	0.15
28.8	1040.8	55.8	56.8	0.097	413.1	0.16
28.7	1037.2	55.6	56.8	0.097	454.9	0.18
28.6	1036.2	55.6	56.8	0.097	475.9	0.19
28.6	1038.8	55.5	56.7	0.097	510.9	0.20
28.6	1043.1	55.5	56.9	0.097	586.4	0.23
28.7	1037.2	55.7	57.0	0.097	535.9	0.21
28.7	1036.2	55.6	56.9	0.097	564.0	0.22
28.8	1033.6	55.5	56.9	0.097	576.8	0.23
28.9	1034.9	55.6	56.9	0.097	529.7	0.21
29.1	1032.1	55.5	56.9	0.097	581.4	0.23
29.0	1034.9	55.5	57.0	0.097	596.0	0.24

Appendix D: Algorithm for Pump and Solenoid Control

The pump controller was controlled used a temperature differential algorithm. The program was developed using NI's development software, labVIEW. The program structure was based on a solid state machine.

The program was split into three states for the pump control that is, the start state (in this instance the default state), pump on state and the pump off. Each state is illustrated below and the logic for activation explained.

Start state, shown in Figure 54 is when the program is 'actively' waiting until its algorithm can be executed. For the activation to occur, three requirements are to be met is firstly, when the collector outlet, T_{co}, is greater than the temperature in the cold region of the tank, T_{tank}, indicating that there is heat to be 'gained' from the collector. Secondly the temperature difference between the collector outlet and collector inlet, T_{ci} is greater than 8 °C. The last requirement is that the temperature in the hottest region of the tank, T_{t1}, needs to be less than 90 °C to avoid overheating.

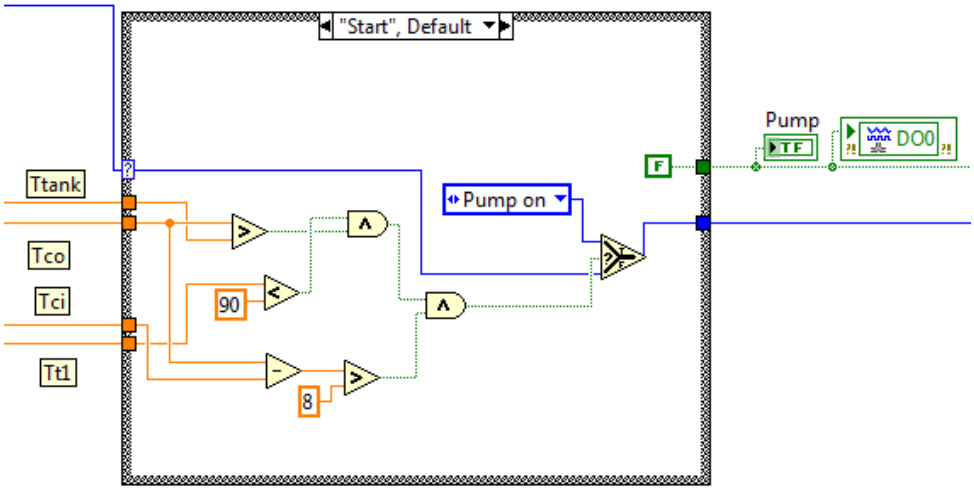

Figure 54: Start state for pump controller

Once these conditions are met the machine moves to the 'pump on' state, shown in Figure 55. When the program enters this state a TRUE signal is sent to the relay to activate the pump. The program then 'actively' checks if the requirements of the algorithm are met. Three requirements are needed, firstly the $T_{co} > T_{tank}$ so that there is always heat gain. Secondly, the inbuilt safety to account for overheating, $T_{t1} < 90$ °C. The last requirement is when $T_{co} - T_{ci} < 4$ °C, when this occurs the program state shifts to the next state.

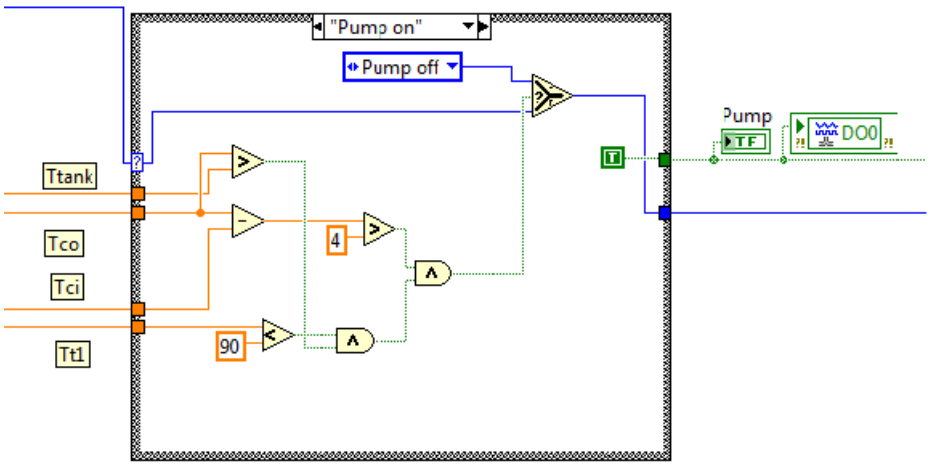

Figure 55: Pump on state for pump controller

The final state, ‘Pump off’’ state sends a FALSE signal to the relay to switch the pump off, shown in Figure 56. The state machine then returns to the ‘Start’ state and the program waits to activate again when needed.

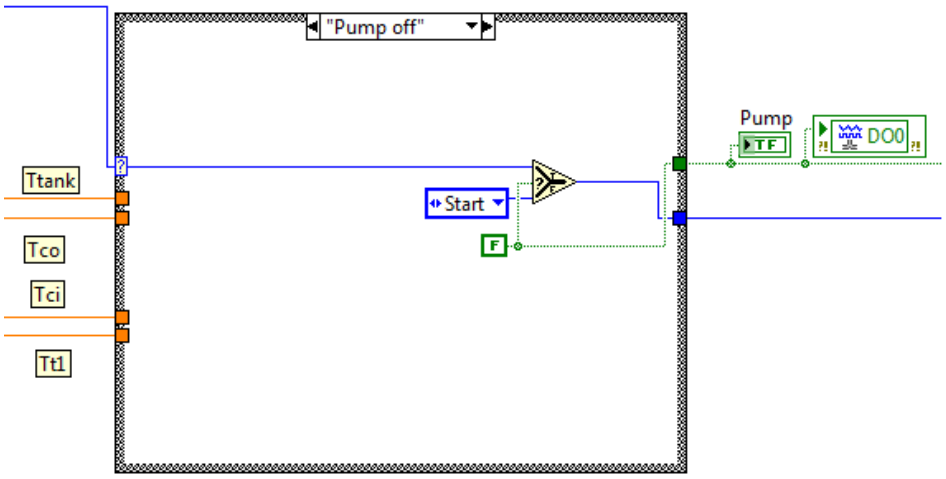

Figure 56: Pump off state of the pump controller

For the solenoid control, a solid state machine program similar to the pump controller was developed; however as can be seen from Figure 57 a more complex algorithm is needed to simulate the load. Unlike the pump controller, which is activated solely on parameters from the system the ‘dump’ controller is activated by the local time and load requirement as set out in the standardised load profile. In summary when a specific time period, requiring a specific load, is activated the program moves to the ‘True’ state where is sends a TRUE signal to the solenoid valve.

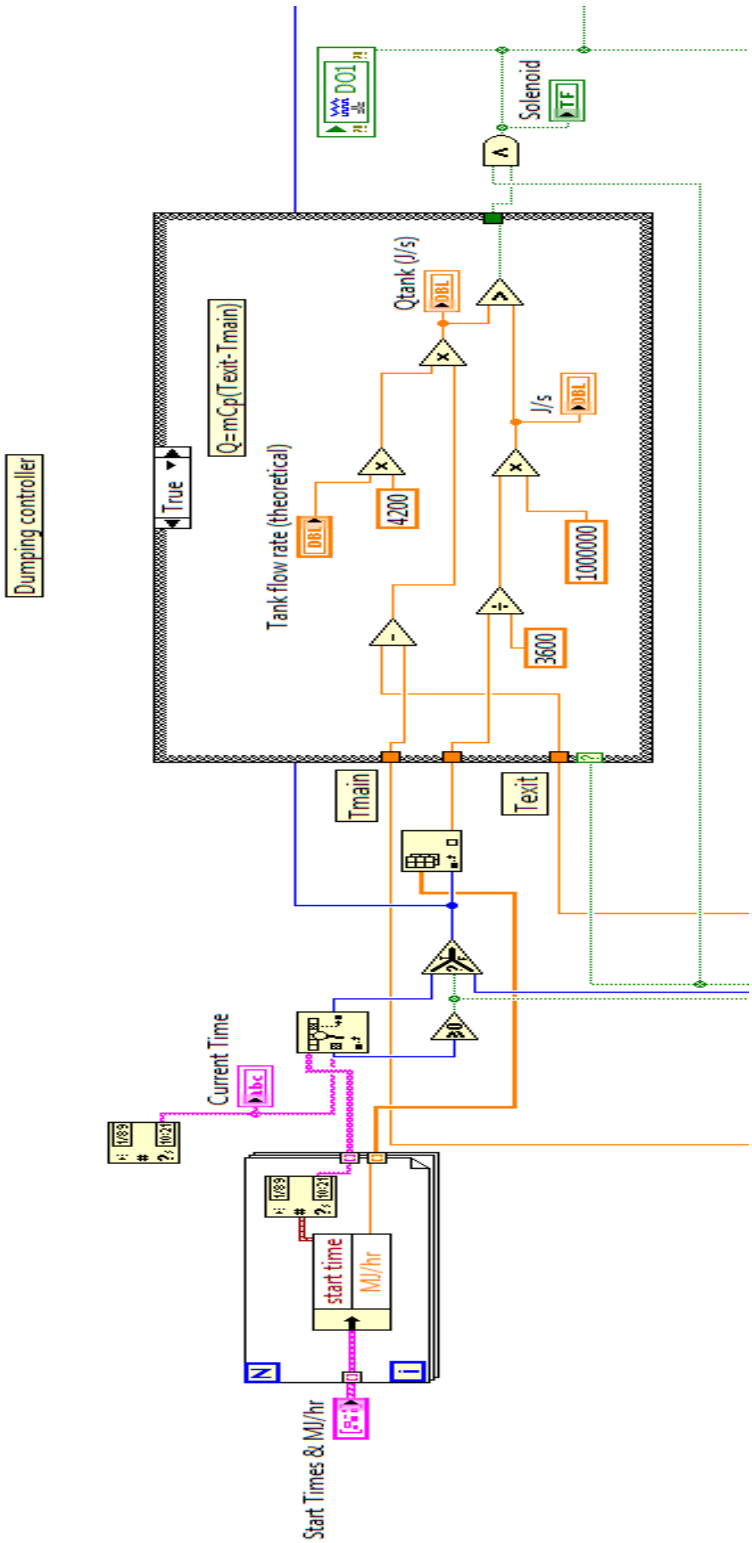

Figure 57: Block diagram of solenoid controller

The program then actively calculates the heat extracted, Q_{tank}, from the tank using Equation 27.

$$Q_{tank} = m\ C_p\ (T_{exit} - T_{main}) \tag{27}$$

Where, m is the flow-out of the tank to the load, C_p is the heat capacity of water and T_{exit} and T_{main} are the outlet and inlet tank temperatures, respectively. The reason for this measure was because the hourly load profile is based on energy required per hour (MJ/hr) as opposed to a certain amount of litres.

When the solenoid is activated by time and required energy, the heat extracted from the tank and energy required are 'actively' compared. Once the required energy is drawn from the tank the controller sends a FALSE signal closing the solenoid and returns to its base state where it waits for the local time to activate is again.

Appendix E: Required Temperature Difference in the Tank to Achieve Required Load

Table 6: Hourly load and required temperature difference

Time	Hourly thermal load (MJ/hr)	Required tank ΔT (°C)
6:00 a.m.	1.13	0.4
8:00 a.m.	3.62	1.4
10:00 a.m.	3.39	1.3
12:00 a.m.	2.49	1.0
2:00 p.m.	1.81	0.7
4:00 p.m.	1.58	0.6
6:00 p.m.	2.49	1.0
8:00 p.m.	2.94	1.2
10:00 p.m.	2.49	1.0
11:00 p.m.	0.68	0.3